Applied Catalysis B: Environmental 198 (2016) 525–547

Contents lists available at ScienceDirect

Applied Catalysis B: Environmental

journal homepage: www.elsevier.com/locate/apcatb

Review

CH_4 conversion to value added products: Potential, limitations and extensions of a single step heterogeneous catalysis

William Taifan, Jonas Baltrusaitis*

Department of Chemical and Biomolecular Engineering, Lehigh University, B336 Iacocca Hall, 111 Research Drive, Bethlehem, PA 18015, USA

ARTICLE INFO

Article history:
Received 13 February 2016
Received in revised form 27 May 2016
Accepted 31 May 2016
Available online 2 June 2016

Keywords:
Methane
Heterogeneous
Catalysis
Direct
In situ

ABSTRACT

Natural gas is envisioned as a primary source of energy and hydrocarbons in the foreseeable future. Though shale gas has recently become abundant, it has two main concerns: its environmental impact and sustainable utilization. The former is the result of recent reports of natural gas emissions and flares into the environment, where it acts as a powerful greenhouse gas, whereas the latter is dictated by the need for efficient hydrocarbon utilization. Modern natural gas processing units that yield clean fuels and feedstock from methane, CH_4, require extremely large capital investments and are not economical in remote natural gas extraction sites. Single step (direct), non-syngas based catalytic routes of CH_4 conversion to value added products have not been competitive economically and need to be reevaluated in the light of shale gas availability. This perspective discusses general considerations for the desired hydrocarbon products, the thermodynamic limitations involved in a single step conversion of CH_4 and heterogeneous catalytic routes based on high temperatures and oxide based catalysts. We then discuss other catalysts and methods of CH_4 activation that have recently emerged and are conceptually different from metal oxide catalyst based routes, such as those using sulfur or halogens. Lastly, we discuss a possible route of CH_4 monetization beyond the first reactive product (such as ethylene oligomerization into fuels), as well as currently explored photo(electro)chemical routes of CH_4 activation.

Contents

* Corresponding author.
E-mail address: job314@lehigh.edu (J. Baltrusaitis).

http://dx.doi.org/10.1016/j.apcatb.2016.05.081
0926-3373/

1. Abundance of natural gas

Natural gas, with its major component CH_4, is and will be in the foreseeable future, the main source of commodity hydrocarbons as well as fuels [1–3]. Total proven natural gas resources alone in 2014 were 6973 TCF (trillion cubic feet) [4] with the U.S. shale gas production projected to increase from 5 TCF in 2010 to 13.6 TCF in 2035 accounting for about half of the total USA dry gas production [5]. Only China, Argentina and Algeria have higher amounts of technically recoverable shale gas: 622.5 TCF as predicted by the Energy Information Administration (EIA). China's proven shale gas reserves are estimated to be 885 TCF – nearly 200 times its annual gas consumption [6]. Finally, methane hydrates, difficult to access crystalline formations containing CH_4, are estimated to account for 317,832 TCF in the USA alone, well beyond the current and future demand [7].

A major shift in the natural gas extraction landscape resulted in new challenges faced by the industry. In the US, extraction wells are situated at remote sites, most of which lack gas distribution infrastructure. Additionally, production from a single well decreases by about 90% during the first few years (Fig. 1**a**), thus necessitating multiple wells scattered across a large area. As a result, large amounts of gas are simply flared into the atmosphere, especially where gas is associated with shale oil extraction. As shown in Fig. 1b about 30% of natural gas in remote North Dakota's Bakken shale is not marketed, but is flared or otherwise lost to the environment [2]. Additionally, recent estimates predict 2300 Gg of methane (0.42% of U.S. gross national gas production) emitted from natural gas production sites due to processing upsets or constraints in infrastructure for transmission and storage [8]. Flaring and venting of associated gas creates negative environmental and public health impacts, while significantly contributing to the potential for climate change [9–13]. For example, the main natural gas component, CH_4, is a 28 times stronger greenhouse gas than CO_2, when a Global Warming Potential (GWP) metric for a 100 year horizon is used. However, since sudden changes are needed to mediate climate change, a 20 year horizon GWP value of CH_4 used is much higher, e.g. 84, to account for its recent abundance and 12.4 year lifetime [14]. An obvious solution would be to reduce the transportation cost. However, the conversion of methane into higher

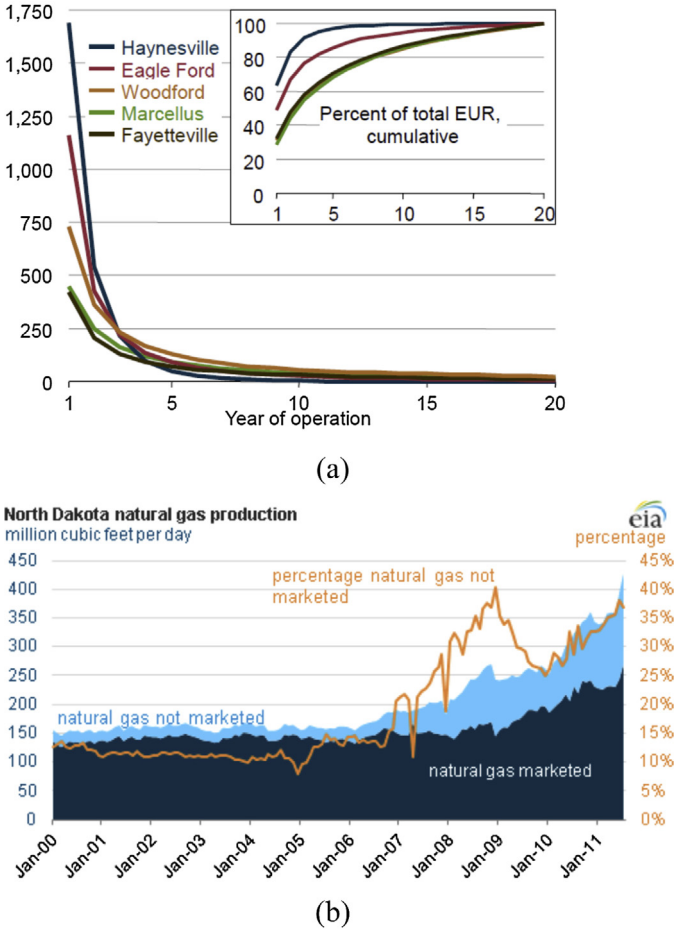

Fig. 1. (a) The average production profiles for shale gas wells in major U.S. shale plays by years of operation (MCF/year) [1]. (b) Projected increased availability of shale natural gas is associated with its large fraction (over 35%) flared (not marketed) [2].

energy density materials and chemical feedstock would prove to be a game-changing answer. This suggests a need for the effective handling of CH_4 at the extraction sites via conceptually novel, low environmental footprint catalytic approaches. In this perspective we focus on heterogeneous catalysis due to its (a) ease of catalyst separation and recycling and (b) high operating temperatures generally necessary to efficiently cleave the strong C—H bond.

2. Desired CH_4 conversion products

Simple reasoning is based on the energy storage capacity of the final product. Information provided in Fig. 2 shows that liquid fuels, such as gasoline or ethanol, have superior energy density (and thus storage and handling) to that of natural gas itself in compressed natural gas form (CNG) or hydrogen fuels, the most used natural gas derived molecule. Liquefied natural gas (LNG) involves cooling down to ca. −160 °C to achieve nearly the same energy density as gasoline or ethanol. Thus, ease of handling suggests the need to convert CH_4 to long chain hydrocarbons (isooctane) and/or lower oxygenates (alcohols). Comprehensive reviews had been done previously by J.H. Lunsford in 1990 and 2000, which basically cover all the conventional methane activation methods [15,16]. The renewed interest in methane activation is also highlighted by the recent review paper by Horn and Schlögl [17].

While various estimation procedures exist on which products would yield the most benefit via direct conversion of CH_4, direct monetary value, volume (market elasticity), as well as to a certain extent environmental impacts, also need to be considered. Table 1 present potential CH_4 activation products, including olefins (ethylene, acetylene), aromatics (benzene, toluene), oxygenates (methanol, formaldehyde, acetic acid, methyl acetate), halocarbons (chloromethane, dichloromethane and chloroform), as well as long chin hydrocarbons, such as distillate fuel oil and gasoline/jet fuel. Due to price fluctuation over time, only approximate numbers obtained in January 2016 are provided. From Table 1 it can be seen that by far the largest market demand is in liquid long chain hydrocarbons for clean fuel production. While of lower demand, ethylene as well as methanol, formaldehyde and acetic acid, are of very high current market value. Halocarbons, while not of very different market value can serve, as indicated in later sections, as convenient intermediates for producing long chained hydrocarbons, using halogens as CH_4 activators. Finally, benzene is used as a raw material for ethylbenzene, which further serves as a precursor for styrene. A widespread use of benzene over toluene in recent years had in fact spurred the use of toluene to form benzene through toluene hydro-dealkylation (HDAL), toluene disproportionation (TDP) and selective toluene disproportionation (STDP) reactions. The HDAL process is indeed an economically challenging process, since toluene has been historically priced above benzene, however, there are still many plants operating for this specific process. HDAL units produce benzene and CH_4; TDP units produce benzene and mixed xylenes; and finally STDP units produce benzene and a *para*-xylene rich stream of mixed xylenes. The reverse HDAL to make toluene or higher methylated aromatics as fuel additive is of direct interest if both CH_4 and benzene are available and will be addressed below. Mechanistically, this problem is very interesting, however, this process is only economically feasible if xylenes can be selectively produced from methane and benzene coupling.

From the data presented in Table 1 it is once again confirmed that of direct interest in CH_4 conversion are lower olefins, oxygenates, cyclic compounds with a varying degree of alkylation. Various combinations of these can then further be catalytically transformed into long chain hydrocarbons to serve as gasoline or jet fuel. Notably, from these only methanol (CH_3OH) and formaldehyde (CH_2O), as well as chlorinated methane (CH_3X) species, contain a single carbon atom while the rest will involve C—C bond formation. As such, they will have to involve both intrinsically the endothermic process of C—H bond breaking and the exothermic process of C—C bond formation providing the first conceptual problem with a single step CH_4 activation process.

3. Current (catalytic) CH_4 conversion methods

Common catalytic processes to activate CH_4 typically follow one of the two approaches, as shown in Fig. 3 [19,20]:

- Direct endothermic dehydrogenation of CH_4 to —CH_2— containing species and H_2 at high temperatures (500–1000 °C). Examples of these are CH_4 aromatization to yield benzene (C_6H_6) and H_2 over Mo-ZSM-5 catalyst and pyrolysis to C_2H_4 and/or C_2H_2 and H_2 [21–23].
- Oxidative (and exothermic) dehydrogenation (or partial oxidation) using O_2 or H_2O as cheap oxidants, as well as other, less used oxidants, such as halogens or sulfur. Examples are partial oxidation of CH_4 to CH_3X (X = OH, Cl, Br or OSO_3H), oxidative coupling to C_2H_6/C_2H_4 and partial oxidation to *syngas* [3,24–26].

By oxidation, CH_4 is converted in refineries into *syngas* with the goal of obtaining H_2 via steam reforming (1) on Ni catalyst followed by the water gas shift reaction (2) to produce more H_2 and CO_2

$$CH_4 + H_2O \leftrightarrow CO + 3H_2,\ \Delta H_r^\circ(298\,K) = 206\,kJ/mol \quad (1)$$

$$CO + H_2O \leftrightarrow CO_2 + H_2,\ \Delta H_r^\circ(298\,K) = -41\,kJ/mol \quad (2)$$

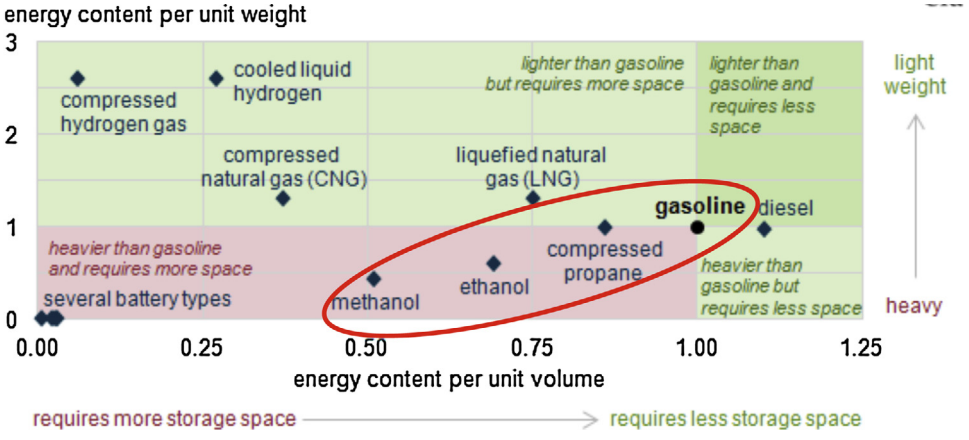

Fig. 2. Energy density comparison of several transportation fuels (indexed to gasoline = 1). Note low volumetric energy density of CNG and compressed hydrogen [18].

Table 1
Tabulated demand for the potential CH_4 conversion products.

Potential CH_4 conversion products	Current Market Value ($ Million)	Price, $/ton	Current Market Demand
Ethylene	194,600	1400	139 million tons in 2014
Acetylene	2200	4400	500 kilo tons in 2014
Benzene	5670	126	45 million tons in 2014
Toluene	1900	100	19 million tons (2020 expected)
Methanol	22,425	345	65 million tons in 2013
Formaldehyde	19,488	420	46.4 million tons in 2012
Acetic Acid	19,560	1200	16,300 kilo tons (2018 expected)
Methyl Acetate	N/A	1080	N/A
Chloromethane	$1401 million in 2012, $1819	350	2 million tons in 2004
Dichloromethane	million (2018 expected)	100	
Chloroform		800	
Hydrogen cyanide	N/A	$370/56 L cylinder	~2000 million pounds in the US
Acrylonitrile	13,000	2600	~5 million tons in 2015
Distillate fuel oil	Very large	Varies	1366 million tons (2012 numbers with 3% annual increase)
Gasoline/jet fuel	Very large	Varies	1269 million tons (2012 numbers with 3% annual increase)

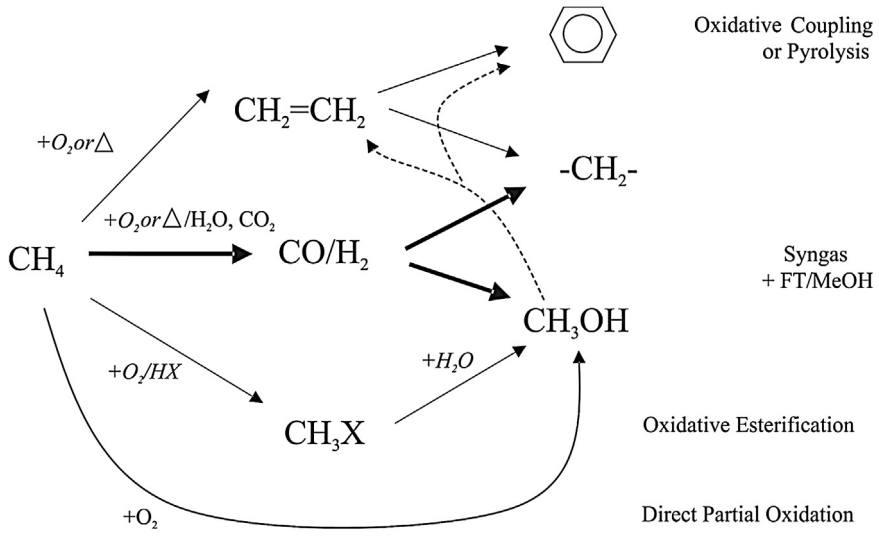

Fig. 3. Conceptual routes of CH_4 activation [19,20].

which results in ~8 tons of CO_2 per 1 ton of H_2 generated. On the other hand, typical large scale gas-to-liquid (GTL) via Fischer Tropsch or CH_3OH routes proceed by a partial oxidation process via slightly exothermic partial oxidation

$$CH_4 + 0.5O_2 \leftrightarrow CO + 2H_2,\ \Delta H_r^{\circ}(298\,K) = -36\,kJ/mol, \quad (3)$$

followed by Co, Fe or Ru based C—C coupling reactions [27]. These catalytic processes generally apply fairly severe conditions to activate the otherwise stable CH_4 molecule, which due to favorable thermodynamics is fully converted into the reactive CO intermediate. As such, *syngas* routes require large catalytic reactors-furnaces with tremendous capital costs due to their technical complexity. The capital costs for GTL facilities reported are very high $110,000 to $200,000/bpd (Pearl GTL and Escravos GTL, GTL projects from Shell and Sasol-Chevron, respectively). For shale gas on remote extraction sites, this scale economy can barely be explored and the complexity of the overall process needs to be significantly decreased via innovative catalytic, preferably single step, processes.

4. Thermodynamic challenge in CH_4 activation

Fundamentally, the main challenge of CH_4 activation while requiring the overcoming of the rather strong C—H bond activation barrier mostly concerns the fact that the desired (intermediate) product is much more reactive than CH_4 itself. Acceptable selectivities are therefore only achieved at low/moderate conversion levels, which result in extensive separation and recycling of unconverted CH_4. *Syngas* based technologies that are presently of industrial significance are based on the premise that *syngas* is thermodynamically favored over CH_4 under reaction conditions of high temperatures and therefore produced at high yield. When reaction (4) is considered for the "deep" hydrogenation of the intermediate product, with CH_3OH on polyoxometalate (POM) and porous organic framework (POF) given as an example,

$$CH_4 + 0.5O_2 \rightarrow CH_3OH \overset{K}{\leftrightarrow} 0.25(CO_2 + 2H_2O) + 0.75\ CH_4$$
$$\Delta G_r^{o}(298K) = -111\ kJ/mol \quad (4)$$

and K for the intermediate product (and targeted CH_4 activation compound) CH_3OH is plotted in Fig. 4, clear limitations of CH_4 partial oxidation reactions, as well as oxidative coupling reactions become apparent with maximum yields of less than 10% [C]. The only processes that fall in between highly efficient syngas partial oxidation (PO) and steam methane reforming (SMR), and those of direct oxidation at low yields, are chlorination and oxy-chlorination. Yields of 30% have been reported for these two processes, possibly due to the stabilizing action of the chlorine atoms via steric hindrance, as confirmed by other bulky hetero groups with the most notable by Periana et al. utilizing H_2SO_4 to obtain CH_3-OSO_3H (methylbisulfate) reactive intermediate at high

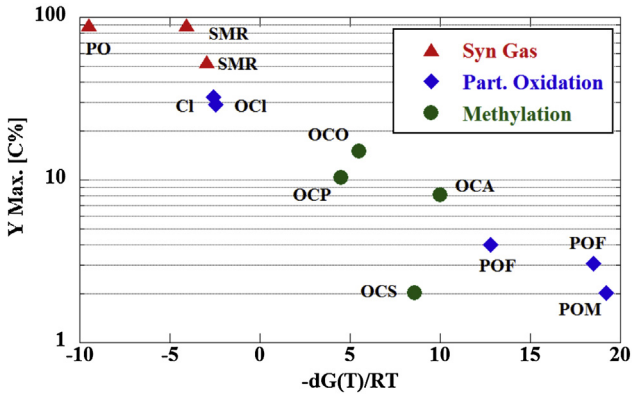

Fig. 4. Thermodynamic limitations of reaction (4). PO – partial oxidation to syngas, SMR-steam reforming to syngas, (O)Cl-(oxy)chlorination, OC(O,P,S,A)-oxidative coupling to olefins, paraffin, acetonitrile or styrene, PO(F,M)-partial oxidation to formaldehyde or methanol. Adopted from Lange et al. [29].

yields [28]. Conceptually, attaching ions larger than Cl^-, such as Br^- or even I^- to activated CH_4. can prevent the newly formed C—Br or C—I bond from further attack thus possibly increasing the single per pass yields. Halocarbon formation from CH_4 as reactive intermediates will be discussed in detail in later sections.

5. CH_4 hydro-de-aromatization (HDA) to form aromatic liquids

CH_4 hydro-de-aromatization (HDA) is of increased interest nowadays due to the recent successful attempts to synthesize seemingly stable catalyst, thus obtaining a stable stream of aromatics and H_2 via

$$6CH_4 \rightarrow C_6H_6 + 9H_2, \quad \Delta G_r^\circ(298\,K) = 428.62\,kJ/mol \qquad (5)$$

The equilibrium conversion for CH_4 at 1 atm and 700 °C is about 12% with about half of the CH_4 going to C_6H_6 and half to naphthalene ($C_{10}H_8$). At 800 °C the equilibrium conversion would be 24% [30]. For comparison, temperatures of ~800 °C are routinely used in steam reforming of CH_4.

Problematically, however, high temperatures thermodynamically favor CH_4 conversion and the catalyst becomes less important due to the radical reactions. In particular, plain silica [31], Fe exchanged silica [22], and molybdenum in ZSM-5 [32] all have been shown to generate cyclic hydrocarbons and H_2. In general, two different schools of thought emerge in catalytic and *in situ* experiments:

- Supported metal oxide clusters (Mo, V, Fe) in ZSM-5, possibly to facilitate cycling hydrocarbon formation [32–34],
- Silica based catalysts [31] that may or not may contain reactive ions, such as Fe [22].

Mo/ZSM-5 catalysts have been shown to work at T = 973 K and atmospheric pressure to yield CH_4 conversion up to 10% and the mixture of gaseous products (selectivity of ~60% towards C_6H_6, 11–20% towards naphthalene and some minor amounts of C_2, as well as sizeable 3–43% of coke) [35]. Identity and anchoring of the isolated oxide species were recently explored using a combination of multiple spectroscopy techniques including *in situ* ultraviolet-visible diffuse reflectance spectroscopy (UV-vis DRS), *in situ* IR and operando Raman spectroscopy, while monitoring gaseous product distribution using a mass spectrometer (MS), as well as theoretical methods via DFT modelling. 2 wt% Mo/ZSM-5 was reduced to oxy-carbide and carbide which seems to be the active phase [23]. Importantly, Mo active sites anchored onto framework Al sites were found more active, e.g. via introducing Al sites via a zeolite synthesis procedure. Sites were re-generable in the presence of O_2 at 773 K C_6H_6 formation is insignificant at all temperatures up to 1000 °C when solid carbon is included in the calculation of equilibrium composition and attempts to mitigate its formation seem to be of particular focus with various oxidants added to the stream [21]. Overall C_6H_6 yields seem to be less than 10%. DFT studies elucidating the reaction mechanism are necessary, although they would have to account for a complex reaction framework proceeding both on the catalyst and as the gas phase radical species.

A remarkable conversion of 32% was observed at 1293 K with major products being ethylene (C_2H_4), $C_{10}H_8$ and C_6H_6 with 53, 25 and 20% selectivity, respectively [22], stable on stream for 60 h. Catalyst has been extensively characterized using XANES measurements and suggested embedded Fe into the silica framework via complex bonding to Si and C atoms. An interesting DFT study was also presented in the same work, where the reaction mechanism comprised CH_3 radical formation at Si—Fe—C_2 catalyst sites and gas phase recombination and chain growth. This is akin to the poor selectivities of most gas phase radical chemistry that is the key for the oxidative coupling of the methane (OCM) process. Most importantly, the temperatures utilized in this work, ~1000 °C, are on the high end for indirect CH_4 activation processes such as SMR and require a large and complex reactor structure and heating methods. The applicability of HDA on remote sites to utilize point sources of natural gas will be difficult to realize instrumentally, while CO_2 emissions will be present to supply necessary heat because the reaction is endothermic. More importantly, on a lab scale, reproducing the results that these authors attained has been very challenging. Auto-thermal heat supply via partial oxidation can be envisioned, but that would drive the system towards *syngas* production.

6. Partial oxidation of CH_4 (POX)

Partial oxidation addresses the severe thermodynamic challenges of the HDA process, which typically takes place at ~500 °C with the desired products methanol (CH_3OH) or formaldehyde (CH_2O) on various catalysts via

$$CH_4 + 0.5O_2 \rightarrow CH_3OH, \quad \Delta H_r^\circ(298\,K) = -126.2\,kJ/mol,$$
$$\Delta Gr^\circ(298\,K) = -111.6\,kJ/mol \qquad (6)$$

$$CH_4 + O_2 \rightarrow CH_2O + H_2O, \quad \Delta H_r^\circ(298\,K) = -282.6\,kJ/mol,$$
$$\Delta Gr^\circ(298\,K) = -287.2\,kJ/mol \qquad (7)$$

although both reactions proceed in the absence of catalyst as well. The inherent reactivities of the CH_3OH and CH_2O products with respect to CH_4 (POM and POF in Fig. 4) result in overall yields of ~2% [20]. These selectivity challenges result when using O_2 for oxidation and no economically viable POX process (especially where CH_3OH or HCHO are the desired products) exists with yields of ~10% often seen as prerequisite for enabling direct POX routes [20]. The use of alternative oxidants (H_2O_2, N_2O and SO_3) is mostly of fundamental importance and fails to be commercialized due to the high costs of these oxidants [20].

6.1. Partial oxidation of CH_4 to CH_3OH and HCHO (POM and POF)

Despite the well-established and robust two step CH_3OH synthesis process via *syngas*, much emphasis has been placed on establishing a single route catalytic pathway. Supported metal oxides (Cu/SiO_2, Cu/MoO_3) [36,37], ZSM-5 encapsulated metal sites (Cu-ZSM-5, Cu-Fe/ZSM-5, Fe-MFI) [38,39], as well as heteropoly-acids (HPA), such as $(NH_4)_6HSiMo_{11}FeO_{40}$, $(NH_4)_4PMo_{11}FeO_{39}$, and

$H_4PMo_{11}VO_{40}$ [40], have all been used in POX. A quick look at these catalysts suggests the presence of specific metals that seem to provide certain activity/selectivity during POX. This series of theoretical and experimental efforts attempted to elucidate the catalysts' molecular and electronic structures that can potentially provide some leads toward further improving these catalysts. In particular, a series of metal-oxy species were investigated with quantum chemical methods utilizing $MO(H_2O)_p^{2+}$ complexes (M = V, Cr, Mn, Fe, Co, $p = 5$ and M = Ni, Cu, $p = 4$) in the gas phase [41]. The rate determining step (RDS) for $CH_4 \rightarrow CH_3OH$ was found to be H-abstraction, which was correlated with the lowest vacant molecular orbital energy of $MO(H_2O)_p^{2+}$. FeO^{2+} was found to be efficient in H-abstraction, but CoO^{2+} and MnO^{2+} were also found to be viable. In general, σ^* controlled reactions presented lower activation barriers than the π^* controlled reactions for a given lowest acceptor orbital energy. The same metals (Cu and Fe, for example) have been utilized in zeolites. Reactive intermediates (of both reactive gas phase molecules and metal catalyst sites) have been explored in sufficient detail using computational and *in situ* measurements. For example, $[Cu_2O]^{2+}$ has been shown to be a Cu/ZSM-5 reactive intermediate via $[Cu_2(O_2)]^{2+}$ precursor by way of combination of resonance Raman, isotope labelling and temperature-programmed desorption (TPD) experiments [42]. Similarly, the structures of Fe active sites in zeolites have been extensively reviewed [43]. Special catalytic sites, so called α-sites, form at 500 °C due to the $Fe^{3+} \rightarrow Fe^{2+}$ reduction and can form α-oxygen that appears to be selective in POM using Fe as well as Cu sites incorporated in zeolites [44]. The major problems appear to be that the CH_3OH formed remains strongly adsorbed on the surface as methoxy, $-OCH_3$, needing a separate extraction/hydrolysis step. Higher temperatures facilitate $-OCH_3$ oxidation to CO and CO_2, thus presenting a big challenge in POX catalyst design. Clear difficulties in obtaining a one step or selective CH_3OH production process even after the extensive amount of experimental and theoretical work suggests the need of alternative catalytic pathways that bypass POX or address product over-oxidation using reactor design, such as product quenching.

On a related note, conversion of 32% with the selectivity towards ($CH_3OH + CH_2O$) of ~28% has been reported at 750 °C on $(NH_4)_6HSiMo_{11}FeO_{40}$ using O_2 as an oxidant [40]. *In situ* analysis of such a complex catalyst system is necessary to understand its exact structure under operating conditions due to the inevitable breakdown of the HPA structure into (reduced) metal oxide counterparts under these temperatures. Nevertheless, HPA can be viewed as an interesting way of preparing active and quite selective POX catalyst.

6.2. Direct formation of acetic acid from CH_4

Recent attempts have been made to form acetic acid (CH_3COOH) in a single step on silica supported Keggin type HPA ($H_4SiW_{12}O_{40}$, $H_3PW_{12}O_{40}$ etc.) at close to room temperature and pressure in the presence of only CH_4, i.e., no expensive catalytic metals such as Pd [45]. The mechanism of C—C coupling, oxygen source to form CH_3COOH and implications for process intensification at these temperatures remain unclear. In contrast, 523–773 K was already used in Zn/H-ZSM-5 to produce CH_3COOH via one step from CH_4 and CO_2 as oxidizer [46]. Zinc appears to be a particularly favorable metal in C—H bond activation [47] of CH_4 via electron-transfer between Zn^{2+} and CH_4 by σ donation from the σ(C—H) orbital of CH_4 toward the Zn 4 s orbital [48]. Selectivity control in these types of reactions is very difficult to rationalize: why would the C—H bond (413 kJ/mol) in CH_4 break before any weaker C—C (347 kJ/mol) and C—O (358 kJ/mol) bonds in CH_3COOH?

Early investigation of the reaction between both thermodynamically stable molecules dates back to Freund's patent [49]. CO_2 and CH_4 were claimed to react over a VIIB or VIII metal catalyst supported on Al_2O_3 or SiO_2 at 100–600 °C with CH_3COOH as the main product. Proof of concept for this reaction was done through separate efforts by Huang et al. [50] and by Wilcox et al. [51]. The latter used temperature programmed reaction (TPR) and *in-situ* diffuse reflectance infrared Fourier transform spectroscopy (DRIFTS) steady-state experiments on Pd and Pt catalysts supported on alumina, while the former studied Cu—Co-based catalysts synthesized by co-precipitation. On Pd and Pt supported on alumina, CH_3COOH was detected while the reaction products in the case of Cu—Co-based catalysts contained various oxygenates including alcohols, aldehydes, ketones, carboxylic acids and even cyclopentane derivatives [50]. Surprisingly, the activation of both relatively inert materials (CO_2 and CH_4) took place at a rather low temperature of 250 °C. The same group subsequently studied three other catalysts, V_2O_5-$PdCl_2/Al_2O_3$, Rh/SiO_2 and Pd/SiO_2 [52,53]. For the former, CH_4 and CO_2 were used as reactants along with O_2 such that the thermodynamics limitation of the conventional reaction could be overcome [52]. Comparison between Rh and Pd revealed that Pd performed better as a catalyst for CH_3COOH formation with 38.38 μmol g^{-1}cat h^{-1} at 200 °C on 2% of Pd, while Rh afforded a lower yield of 12.26 μmol g^{-1}cat h^{-1} at 400 °C [53]. In this particular study the reactant flow was alternated with pure CH_4 flow for a fixed amount of time followed by pure CO_2 for a longer period of time. This method significantly improved the reaction outcome which is explained by the initiation with CH_4 dissociation to the methyl radical ($^{\bullet}CH_3$) followed by CO_2 insertion [53]. DFT simulations in the gas phase were also carried out to confirm the reaction mechanism [54]. It followed that the reaction can proceed via two different pathways, e.g. via CO_2^- or CO, with the former being more favorable. The pathways also involved dissociation of CH_4, which, in addition to CO_2^- anion formation, was the rate limiting step [54].

In relation to the previously discussed Zn effects on CH_4 activation, a recent study on Zn/ZSM-5 using ^{13}C MAS NMR spectroscopy revealed the dissociation behavior of CH_4 [55]. On fully-doped ZSM-5 surface sites, where there are no Brønsted acid sites, adsorption of CH_4 alone yielded Zn-CH_3 species at $T \geq 523$ K, whereas on partially substituted zeolites (60% Brønsted acid sites), $-CH_3$ readily formed at room temperature. The methyl species was further converted into the $-OCH_3$ species when oxygen was introduced into the system. The importance of Brønsted acid sites was also acknowledged in the case of Cu-exchanged ZSM-5 and mordenite, where without Brønsted acid sites, i.e. fully substituted catalyst, there was no product detected at low temperatures [56]. Confirmed by EPR, Na titration and ^{13}C MAS NMR spectroscopy, Cu_xO_y played an important role by dissociating CH_4, which was followed by $-CH_3$ spillover to the support and formation of the $-OCH_3$ species. In this case, the introduction of CO and water subsequently led to the formation of CH_3COOH. This indicated the shared effect of both dopant and support. Zn facilitated CH_4 dissociation, while the support played an important role in the carbonylation step. Cu-MOR was more selective than Cu-ZSM-5, generating 22 μmol/g cat as opposed to 4 μmol/g cat [56]. While attractive from a practical perspective of converting two greenhouse gases (CH_4 and CO_2) into CH_3COOH, the very low process efficiencies are prohibitive and no clear path for the process intensification was apparent.

7. Oxidative coupling of CH_4 (OCM)

As discussed, a single-step catalytic conversion of CH_4 can proceed via endothermic dehydrogenation but is very thermodynamically limited. On the other hand, single-step catalysis involving POX using oxygen containing oxidants suffers from selectivity issues. One of the most promising methods of adding value to CH_4 via a single step catalytic reaction is OCM to form high value (~$1000/ton) and high demand (~140 Mton/year) product

ethylene, C_2H_4, a vital building block in the chemical industry via reaction (8)

$$2CH_4 + 0.5O_2 \rightarrow 0.5C_2H_4 + H_2O,\ \Delta Hr^{\circ}(800\,^{\circ}C) = -139\,kJ/mol,$$
$$\Delta Gr^{\circ}(800\,^{\circ}C) = -153\,kJ/mol \quad (8)$$

It is a direct and exothermic process not constrained by thermodynamic limitations, such as those in CH_4 hydrodearomatization (HDA) to form aromatic liquids. It is imperative that this partial oxidation reaction be controlled by the catalyst kinetics since thermodynamics competes with oxidation to form CO_2 and is more favorable via reaction (9)

$$CH_4 + 2O_2 \rightarrow CO_2 + 2H_2O,\ \Delta Hr^{\circ}(800\,^{\circ}C) = -801\,kJ/mol,$$
$$\Delta Gr^{\circ}(800\,^{\circ}C) = -801\,kJ/mol \quad (9)$$

Practical, active, selective and stable catalysts for reaction (8) have not been obtained to date, although hundreds of materials have been tested [57,58]. The only thermally very stable known catalyst system that yields a promising, although insufficient, CH_4 conversion of 20–30% and C_2 selectivity of 70–75% is supported $Mn/Na_2WO_4/SiO_2$. The catalytic data obtained to date relied on combinatorial synthesis/screening methods rather than structure-property relationships, thus, inhibiting its rational design from fundamentals. In fact, as discussed below, there is virtually no information on the nature of the catalytic active sites involved, as well as the fundamental reaction data governing their kinetics and selectivity. In addition to that, there are several engineering challenges that need to be overcome. As pointed out above, this reaction is of extreme exothermicity, which creates concern of heat management. Secondly, the use of air is not feasible in this case, and pure O_2 also creates another potential economic hurdle. Finally, the location of the OCM plant should concern the values it creates, i.e. the remote gas sites might not be of feasible location. Siluria [59] is currently attempting to commercialize an OCM process, but catalyst details are not known. Fundamental insights about the catalysts could potentially assist economically feasible development of this process.

7.1. Current understanding of supported $Mn/Na_2WO_4/SiO_2$ OCM catalysts and associated fundamental issues

There is lack of descriptive studies in the catalysis literature that clearly define the structure of the catalytic site(s), their specific roles (active or spectator), as well as the role of the promoters used, such as Mn and Na during OCM. An extensive literature search was summarized [58] as shown in Fig. 5 and yielded several widely different descriptions of the surface active sites and their role during OCM by supported $Mn/Na_2WO_4/SiO_2$: (1) a redox mechanism involving $W^{6+} \leftrightarrow W^{4+}$ redox couple of surface dimeric —[WO_3—O—WO_3]— units was suggested and gas phase O_2 was proposed to be involved in electron transfer from W to the vacancy forming the F-center (Fig. 5a) [60]. This model was based on *ex situ* EPR spectroscopy measurements at low temperatures, but neither W^{6+} nor W^{4+} are paramagnetic, which makes them EPR silent, and there is no supporting data for the presence of dimeric W_2O_7 sites in the catalyst. Further, F-centers are thermally unstable in the presence of O_2 so their role, if any, remains unclear; (2) CH_4 activation on a W^{6+} site with O_2 activation on the neighboring Mn^{3+} site with oxygen spillover accomplishing the reactive cycle (Fig. 5b) [61]; and (3) the bridging Na—O—Mn bond was proposed as an active site due to the similarity between the catalytic performance of $Mn/Na_2WO_4/SiO_2$ and Na_2MnO_4/SiO_2 with W only preventing Na loss [62]. The Na was also proposed to moderate Mn-WO_4 interactions by affecting reducibility of the latter [63]. Finally, there are two distinct cristobalite (active OCM catalyst support) phases that depend on temperature: α-cristoballite is thermodynamically favored below 250 °C while β-cristobalite is present at higher temperatures [64]. The literature, however, only reports detecting the α-phase because all prior analyses were performed on catalysts cooled down to room temperature [65–67].

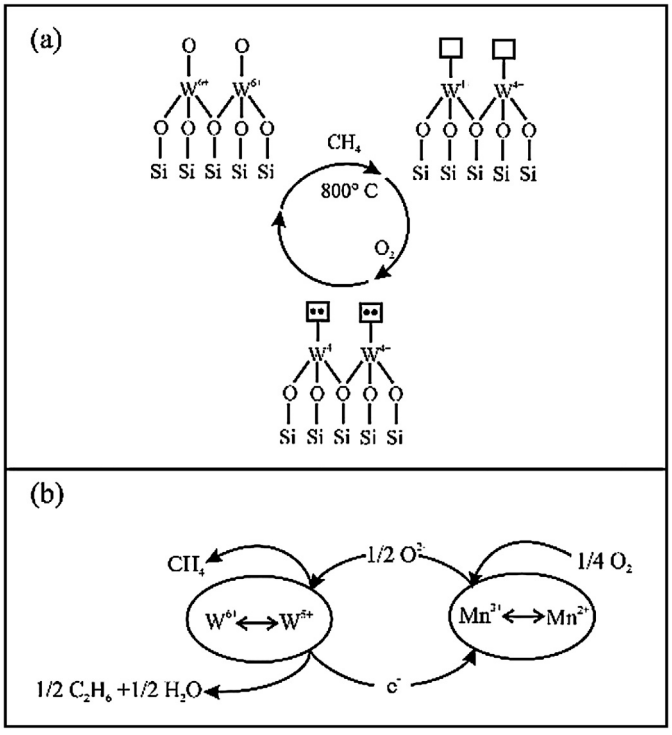

Fig. 5. Literature proposed surface active sites and CH_4 transformation mechanisms on $Mn/Na_2WO_4/SiO_2$ during OCM [58].

None of these studies, however, attempted to elucidate mechanism or active site structure with direct spectroscopic measurements under reaction conditions. The dynamic structural changes of the catalysts from room temperature-air exposed samples to reaction temperatures at 800–900 °C under OCM reaction conditions are dramatic and, thus, ambient characterization will not reflect the structures under reaction conditions. Consequently, future research should focus on elucidating the structure-reactivity relationship of the most active supported $Mn/Na_2WO_4/SiO_2$ OCM catalyst and apply the new fundamental insights that will be gained for the rational design of advanced SiO_2-supported W, Mn and Na promoted model catalysts capable of enhancing overall yields of C_2 products. Once the functions of Mn, Na and W for OCM are established, they can be substituted by other oxides possesses corresponding desirable characteristics.

7.2. Ethylene oligomerization

A route to address higher hydrocarbon demand can be conceptualized utilizing ethylene (C_2H_4) produced via CH_4 OCM. It would involve generation of C_2H_4, separation and recycling of the remaining gases followed by C_2H_4 oligomerization

$$CH_4 \xrightarrow{OCM} C_2H_4 \xrightarrow{oligomerization} C_4 - C_{20} \quad (10)$$

(Homogenous) C_2H_4 oligomerization is a well-researched reaction developed by Shell (SHOP), Chevron-Phillips Chemical Company and British Petroleum [68]. There are several highly active homogeneous catalysts for the selective C_2H_4 oligomerization,

namely PNP, PCNCP, NPN, Mer-coordinating tridentate and Fac-coordinating tridentate ligands. The PNP system, without any metal dopants was able to catalyze either trimerization or tetramerization of C_2H_4 depending on the catalyst finetuning that involved modification of *ortho*-substituents of the phenyl ($-C_6H_5$) groups, alteration of catalyst backbone and substitution of a $-C_6H_5$ group with phosphine or amine [68]. On the second system, a chromium metal center was supported by PCNCP ligand with only the phosphines bind to Cr. In this particular system, yield of C_6 was reported to be as high as 97% with alkene selectivity of 95% while 99% of the produced C_8 (yield = 1%) is 1-octene. The rest of the homogenous catalysts class mentioned above also involves the addition of Cr metal site to the supporting ligand. SHOP catalysts, however, involve the use of Ni metal eliminating the need of using other transition metals in combination with aluminum co-catalysts [69]. This is due to so called "nickel effect" when nickel salts modify the nature of the oligomerization products from α-olefins to 1-butene [69]. Homogeneous catalysis has helped investigators to understand the general mechanistic aspects of product control during C_2H_4 oligomerization giving a starting point for developing the heterogeneous counterparts for a potentially successful CH_4 monetization using this route. This is of utmost importance in realizing a low separation cost heterogeneous catalyst oligomerization process not commercially utilized currently.

7.2.1. Heterogeneous catalysts for ethylene oligomerization

Three groups of heterogeneous catalysts have been extensively investigated for C_2H_4 oligomerization reaction, all of them intuitively focused on nickel-based catalyst supported on silica-alumina [70–80]. The logic behind it is that zeolites can easily oligomerize propylene (C_3H_6) and other higher olefins, while nickel-based catalysts are known to dimerize C_2H_4. The homogeneous catalysis, however, is still much more superior to its heterogeneous counterpart with the reactions highly selective and leading to the formation of mostly 1-alkene. Although heterogeneous catalysis could lead to the formation of hydrocarbon with even number of C atoms, such as C_4—C_{12}, the heterogeneous oligomerization is non-selective leading to the distribution of isomers. This is highly likely due to the lack of control in structural and compositional distribution of the catalytic surface sites requiring their detailed *in situ* investigation.

7.2.1.1. Ni exchanged silica-alumina materials. Silica-alumina supports, ranging from thermally synthesized silica-alumina [71,72,80], MCM [73,74,76,77], zeolites [75,79] and Al-SBA [70,78] were studied to date with metal doping carried out by either impregnation or ion-exchange. Tuning this catalyst system mainly focuses on the structure of the support [70,71,74,78] and/or optimizing the Si/Al ratio leading to a varying acidity [73,74,80]. The best performing catalyst was found to be prepared by alumination of silica via grafting sodium aluminate onto pure SBA-15 and ion-exchanging the support subsequently [70]. This effort lead to a unique molecular structure of the support where a network of interconnected mesopores was large enough to allow the free diffusion of products resulting in superior activity of 175 g oligomer/g_{cat} hand lower deactivation rate, when tested using both batch and fixed bed reactors [70]. Conversion of the raw material was high (up to 99% of C_2H_4 [71]). However, the product distribution was still mediocre where in one case, the yield of 1-hexene was 13.4%, as compared to >90% in the case of homogeneous catalysis [80].

With low heterogeneous catalyst selectivity in mind, Hulea's group published their first work on Ni-exchanged Al-MCM-41 catalyst. The catalyst support was synthesized by autoclaving gels of the precursors (NaOH, $NaAlO_2$, CTABr, and SiO_2), drying and calcining the obtained solid and ion-exchanging it with ammonium nitrate, $NH_4(NO_3)$, followed by nickel nitrate, $Ni(NO_3)_2$. Tested in a slurry reactor, all catalyst showed great selectivity toward oligomers of even number (C_4—C_{10}) but lower acidity catalysts presented higher activity and stability. The isomer selectivity within the same class of products, e.g. C_4, C_6, C_8 or C_{10}, however, remained a problem [73]. Subsequently, these catalysts were studied using DRIFTS by means of CO-probing and the active sites were found to be both Ni^{2+} and Ni^{+} ions where the latter was formed when the catalyst was thermally activated under dry atmosphere [76]. This group also studied two other zeolitic materials as the support, namely dealuminated Y zeolites as well as MCM-36 and MCM-22 [74,75]. The two MCM catalysts were synthesized hydrothermally from a gel containing the precursors while the dealuminated Y zeolites were procured commercially. The method of doping was similar to that of MCM-41, e.g. by subsequent ion-exchanging of ammonium and nickel. The Y zeolite catalysts significantly lower the reaction temperature operating at 30–70 °C, when compared to MCM-41, with high activities of 16–30 g oligomer/g_{cat} h. Higher reaction temperature, however, led to the increase in higher alkene production [75]. Comparison between the two MCM catalysts showed that catalyst with mesoporous structure and mild acidity (MCM-36) possessed higher activity and selectivity than that of microporous structure and high acidity (MCM-22) [74]. The latest catalyst studied by this group was prepared by alumination of silica by grafting sodium aluminate onto pure SBA-15 and subsequently ion-exchanging the support [70]. This particular catalyst possessed a unique structure with the network of interconnected mesopores large enough to allow the free diffusion of products leading to almost three times the activity of the Ni/Al-MCM-41 catalyst (175 g oligomer/g_{cat} h compared to 62 g oligomer/g_{cat} h) and lower deactivation rate tested on both batch and fixed bed reactors [70].

The Al-SBA-15 support was also investigated by Lin et al. [78]. On the synthesized catalyst, steam, alkali and acid posttreatments were conducted. The synthesized support had plug morphological structure and acid treatment at low temperatures led to the formation of higher surface area and pore volume material while at higher temperature, blocked the plugs in the catalyst preventing intermediates to be desorbed and transported [78]. The latter, along with steam-treated catalyst, exhibited improved selectivity towards C_{16} owing to its shape selective structure. Another studied support for Ni was H-beta zeolite, investigated by Martinez et al. [79]. In their study, both ion-exchange and impregnation were investigated leading to 87% C_2H_4 conversion using Ni content of ca. 5%. However, this support did not exhibit high selectivity giving a mere 40–70% of C_4 and even lower for higher alkenes while also sacrificing the conversion down to 10–30%. Interestingly, their IR experiments ruled out Ni^{+} as the active site, contradicting Hulea group's findings [79].

7.2.1.2. Metal oxide supported NiO and $NiSO_4$. Long before the Ni-exchanged silica-alumina catalysts were developed, supported NiO and $NiSO_4$ were investigated as the first heterogeneous catalyst. Similar to the Ni-exchanged silica-alumina, the acidity of the support played a major role in the catalyst activity and selectivity. Different supports have been tried (Al_2O_3, TiO_2, ZrO_2, WO_3, MoO_2) and fine-tuning the system heavily depended on the acidity of the support. More details on these systems had been reviewed by Finiels et al. [81]. Supported NiO and $NiSO_4$ exhibited a remarkable selectivity towards C_4 oligomers at 20 °C with moderate TOFs of 5–30 h^{-1} with Ni content much higher (4–36 wt%) than in the Ni-exchanged on silica-alumina materials (0.6–5 wt%). This catalyst loading/product distribution duality implies different active catalytic site structure and the resulting functionality but did not receive sufficient experimental attention, as shown below.

7.2.2. Nature of the active sites and reaction pathways on supported Ni catalysts for C_2H_4 oligomerization

7.2.2.1. Active sites for C_2H_4 oligomerization. There have been conflicting reports regarding the nickel species responsible for the C_2H_4 oligomerization [76,79,81]. While NiO has been ruled out as the catalytic active site, Ni^0, Ni^+ and Ni^{2+} have been proposed to be the active sites of the reaction [81–84]. EPR/ESR and CO FTIR were the two techniques addressing the catalytic active sites [85–88]. From ESR, Choo et al. concluded that Ni^+ was the active species [85], a view also shared by Kermarec et al. [88]. Recent *ex-situ* characterization of the Ni/Al-MCM-41 revealed that both Ni^+ and Ni^{2+} assume similar roles in catalyzing the C_2H_4 dimerization [76]. However, this view has recently been challenged by Martinez et al. who argued that only Ni^{2+} was the active site [79]. This controversy originated from the fact that all these characterizations were done *ex-situ*; no *in-situ* experimental work has been done to analyze this reaction. To summarize, the effect of acidity of the support rather than chemical (and structural) state of the nickel active site are well known.

7.2.2.2. Reactive pathways in heterogeneous C_2H_4 oligomerization. Unlike the homogeneous catalysis where the proposed reaction mechanisms are highly debated, the reaction pathways for the heterogeneous counterpart have fewer contradictions. Summarized in the recent review by Finiels et al., there are three reactions in the overall mechanism [81]. Nickel active sites assume the role as the catalyst for the first reaction, where the metal site opens up the olefin's double bond and further acts as a center for insertion of the subsequent molecules initiating coupling between those C_2H_4 molecules. Co-oligomerization and isomerization then take place over the acid sites with C_4 and C_6 olefins consumed involving carbenium ions leading to the formation of higher olefins, both linear and branched. Higher olefins can then convert into coke or crack to yield smaller molecules [81]. Only recently, however, some computational work focused on Ni/SSZ-24 revealed that the Cosse-Arlman mechanism, the originally proposed mechanism for homogeneous catalysis where a vacant coordination site on a metal atom opens up the double bond to initiate polymerization of C_2H_4, was the main pathway for the dimerization with Ni^{2+} as the active site [89]. An idealistic single Ni atom active catalytic site has been used in this work based on the assumptions stemming from a single site homogeneous C_2H_4 oligomerization work. However, the absence of any *in situ* work to determine the exact nature of this active site clearly calls for another interpretation of the reactive mechanisms, especially important in determining and possibly controlling the selectivity of the heterogeneous C_2H_4 oligomerization.

8. Non-oxygen catalysts and oxidizers for CH_4 activation

Non-oxygen routes have in general been avoided due to the (a) introduction of chemical compounds other than oxygen, (b) catalyst costs and (c) resulting separation and product contamination issues. However, in principle they can be CO_2-free thus having a transformation impact environmentally. Additionally, they can address a critical issue of over-oxidation, pervasive when using O_2 as an oxidizer. Oxidative approaches that apply oxidants other than O_2, e.g. Cl_2, H_2SO_4/SO_3, H_2O_2 and super acids, so far failed to become widespread mostly due to the high cost of the oxidant. Additionally, all of these need to be regenerated with O_2 resulting in additional processing steps and byproducts. We wll revisit that later during the discussion of confining the oxidizers to a solid form.

8.1. Sulfur as an abundantly available oxidant for CH_4

While conventional and shale gas resources are mostly sulfur free, some of the accessible natural gas fields contain tremendous amounts of so called sour gas, e.g. H_2S and/or CO_2. In fact, explored gas reserves that contain 1–15% and more than 15% of H_2S comprise 30.1 and 4.9% of the total available natural gas reserves, respectively [90]. For example, the Bab Sour Gas project in UAE will process 1 bcf of sour natural gas per day containing up to 33% H_2S. The UAE holds the seventh-largest proven reserves of natural gas in the world, at slightly more than 215 trillion cubic feet (TCF) [91]. Despite this, the UAE became a net importer of natural gas in 2008. This phenomenon is a result of two things: (1) the UAE reinjected approximately 30% of gross natural gas production in 2012 into its oil fields as part of enhanced oil recovery (EOR) technique, and (2) the country's rapidly-expanding electricity demand fueled by the economic and demographic growth of recent decades-relies on electricity from natural gas-fired facilities. Some 9200 tons/day of elemental sulfur are produced via the Claus process from H_2S on a single Shah, UAE, gas field alone providing for an inexpensive and abundant material onsite. At this point, the presence and opportunities in the catalysis of CH_4 via (a) the mixed $CH_4 + H_2S$ streams and (b) using elemental sulfur as a soft oxidant will be discussed.

8.1.1. CH_4 reforming with H_2S

This is a single step route that involves generating useful products from CH_4 and H_2S mixtures, including CS_2 (recently proposed as a solvent for EOR [92,93]) and H_2 via

$$CH_4 + 2H_2S \rightarrow CS_2 + 4H_2,\ \Delta G_r^\circ(298\,K) = 184.94\,kJ/mol. \quad (10)$$

While intrinsically endothermic and a high temperature process, in principle it will not generate CO_2, typical in reactions involving oxygen containing oxidizers (H_2O, O_2). It could also serve as an alternative to the Claus process, where H_2S is disposed of as elemental sulfur and H_2O via combustion with O_2. So far, work for this reaction has focused on the investigation of the thermodynamics of the process in order to minimize solid carbon deposition. With an excess of H_2S, temperatures of >1000 °C are necessary to have a solid carbon-free process [94], putting a tremendous constraint on the catalyst design to accelerate the kinetics of this process. A very recent work [95] devised Fe_2O_3/γ-Al_2O_3 materials for this particular reaction via sol-gel impregnation with iron nitrate solution. They operated for 14 h with 100% CH_4 conversion and ~60% H_2S conversion at 1:12 CH_4 to H_2S molar ratio. Selectivity of the catalyst towards CS_2 was linked to Fe^{3+} ions in octahedral coordination of hematite (α-Fe_2O_3), which is highly unlikely in the presence of the reducing stream and very high temperatures. In addition, Cr_2S_3 and Ce_2S_3 have been used for the same reaction with a molar CH_4/H_2S feed ratio of 4 and a variable residence time from 1 to 5 s [96]. No *in situ* characterization of catalyst is present for these materials under the operating conditions of CH_4/H_2S and the catalytic site structure is of big interest, as well as the steady state performance. No measured kinetics are also available to the authors' knowledge.

8.1.2. Methyl mercaptan (CH_3SH) route of sour gas to olefins, BTX and hydrocarbons

CH_4 reforming can also proceed using elemental sulfur rather than H_2S although the overlap between the mechanisms at these high temperatures cannot be ruled out. This multi-step conversion process can be initiated by the catalytic reaction of CH_4 with elemental sulfur to selectively yield CS_2 and H_2S via

$$CH_4 + 4S \rightarrow CS_2 + 2H_2S,\ \Delta G_r^\circ(298\,K) = -902.3\,kJ/mol \quad (11)$$

This step can be performed by reacting preheated CH_4 in the mixture with vaporized elemental sulfur at 580–635 °C and pressure of 2.5–5 atm in an adiabatic reactor (Folkins process). Details of various catalysts have been reported for this reaction, including silica, alumina, magnesia, metal oxides and sulfides [97]. Consecutively, CS_2 hydrogenation via

$$CS_2 + 3H_2 \rightarrow CH_3SH + H_2S \quad (12)$$

with H_2 obtained via CH_4 reforming with H_2S discussed in the previous section is performed. This catalytic reaction has extensively been covered and validated recently by Johannes Lercher and coworkers [98,99]. Ni-, Co- and K-doped MoS_2 supported on SiO_2 were used and 100% conversion of CS_2 was achieved with 100% CH_3SH yield at 550 K on $CoKMoS/SiO_2$ [99] with $H_2/CS_2 = 5.9$ and GHSV = 89.2 min^{-1}. Adding potassium to the catalyst was shown to decrease the rate of CS_2 hydrogenation, whereas temperatures above 550 K resulted in formation of CH_4 as byproduct. The catalyst was stable on stream with MoO_2, MoS_2 and K_2SO_4 detected via XRD. The latter was proposed to inhibit conversion of CS_2, as it is difficult to reduce. The chemical state and binding to the active elements and the substrate of potassium ions is particularly puzzling as most of the potassium species appear to be inactive in this process. Some detailed quantum chemical investigations would be able to explain K-promotion effects on sulfur containing carbon compound catalytic transformations.

The resulting CH_3SH can be considered as an activated methane species (CH_3—SH) that is isostructural with CH_3OH. Attempts have been made to perform catalytic coupling of CH_3SH into higher hydrocarbons, as shown in Fig. 6, utilizing the knowledge and the catalysts available for CH_3OH reactions via

$$CH_3SH \xrightarrow{CHA,ZSM-5} 1/n(CH_2)_n + H_2S \quad (13)$$

Very few attempts have been made of CH_3SH catalytic coupling to obtain lower olefins, when compared to the industrial expertise with CH_3OH conversion. Chang and Silvestri [100] reported that at 755 K using H-ZSM-5 catalyst CH_3SH was converted into H_2S and a mixture of hydrocarbons with 7.0% selectivity towards lower olefins with 27.2% of the feed carbon converted to dimethylsulfide (DMS). Butter et al. [101] claimed high CH_3SH conversion to CH_4 at 531 K on H-ZSM-5. Mashkina et al. [102] identified the presence of CH_4 when CH_3SH was processed on various acid catalysts between 623 and 673 K, while at lower temperatures DMS was the only product at equilibrium conversion. Formaldehyde was one of the value added products when CH_3SH was partially oxidized on 1 wt% V_2O_5/TiO_2 catalyst with maximum selectivity towards CH_2O achieved at 400 °C [103]. A very recent work (2013–2014) by TOTAL SA focused on the catalytic conversion of CH_3SH on acidic zeolites [104–106] and showed the absence of lower olefins but with few mechanistic explanations provided. In particular, large amounts of (a) CH_4, (b) DMS, (c) coke and (d) and no lower (C_2=, C_3=) alkenes were observed, in addition to BTX (benzene, toluene, xylene) products formed. This is surprising since olefins are typically considered to be precursors to BTX formation [16]. It is possible that since CH_3SH catalytic condensation was attempted at temperatures higher than those for CH_3OH (823 K vs 623 K) with any C_2H_4 formed further reacted on very strong acidic zeolite sites to yield coke and CH_4. Instead, moderation of the acid site strength in metal doped HZSM-5 has been shown to increase selectivity towards C_2H_4 [107] and can be performed in future work. Acidic supported $WO_x/\gamma\text{-}Al_2O_3$ catalysts previously shown to partially form C_2H_4 from CH_3SCH_3 by Olah et al. [108] can also be potentially used for CH_3SH coupling reactions as well as Ru, Co or Fe,

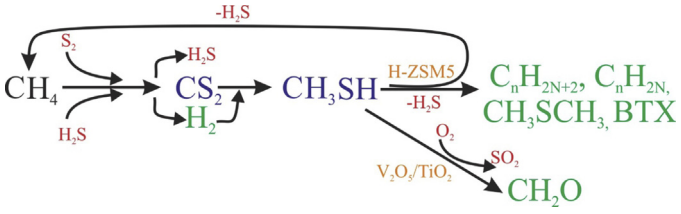

Fig. 6. Methyl mercaptan (CH_3SH) intermediate based routes of CH_4 transformations into value added products.

which are expected to reduce catalyst acidity and improve selectivity towards olefins [107]. Provided the poor selectivity of CH_3SH coupling only very few attempts to analyze the fundamental mechanistic steps to form lower olefins in chabazite were investigated. This was done using quantum chemical methods only very recently and did not provide a direct route to C_2H_4 based on three classical mechanisms (associative/dissociative/oxonium) [109]. It is clear that CH_3SH route of CH_4 activation, involving consecutive steps, can benefit specific highly sour gas fields in yielding high value products.

8.1.3. Sulfur as a "soft" oxidant for CH_4

A single step conversion of CH_4 to higher hydrocarbons (C_2H_4 and C_2H_6) was found to be accelerated when sulfur and/or chlorine were added to the catalyst material resulting in a very complex catalyst composition, such as Co/Zr/S/P/Na/K/Cl/O at 500 °C and 1:1 CH_4 to O_2 ratio [110], e.g. still requiring oxygen to proceed via OCM. The addition of sulfur and chlorine to methane has remained interesting. However, only recently have the fundamentals of sulfur and chlorine addition been fully explained. The CH_4 coupling reaction using sulfur, not oxygen, as an oxidant via

$$2CH_4 + S_2 \rightarrow C_2H_4 + 2H_2S, \quad \Delta G_r^{\circ}(1073\,K) = -4.90\,kJ/mol \quad (14)$$

is exergetically favorable at temperatures above 950 K and the complete "overoxidation" into CS_2 is less exergetic when compared to its oxygen counterpart, CO_2. Yet early attempts have been made to use S_2 vapor as an oxidant on metal oxide catalysts, such as Sm_2O_3 [111] or complex oxygen based catalytic systems, such as Mo—V—Cu—P—O, W—Pb—B—O, V—Zn—Bi—B—O at 670–560 K [112]. Only very recently has a distinct study combining fixed bed reactor and quantum chemical calculations reported CH_4 coupling with S_2 on unsupported and ZrO_2 supported metal sulfide catalysts (with the latter used to disperse the active catalytic material) [25]. CH_4 conversion of 16% was reported with ~20% C_2H_4 selectivity at 1323 K, 5% CH_4 in Ar, CH_4/S ratio of 5.8, stable on stream for at least 24 h. First principles calculations indicated that stronger metal-sulfur bond compounds (PdS, TiS_2 and substoichiometric $Pd_{16}S_7$) had higher C—H bond activation energies but lower —CH_2— coupling activation energies thus enhancing C_2H_4 selectivity (and CH_4 conversion expense). Altering WHSV in these experiments also followed a typical trend with large WHSV values decreasing CH_4 conversion and improving C_2H_4 selectivity (less overoxidation). While interesting and showing truly novel fundamental insights in "soft" oxidation of CH_4, these experiments produce worse C_2H_4 yields than during the regular OCM, while mechanistic details on the catalysts are difficult to decouple from the gas phase (radical) reactions concurrently proceeding at these high temperatures.

8.2. Halogen based CH_4 activation routes

Halogen based CH_4 activation routes generate MeX (Me = CH_3; X = Cl, Br or I) intermediates that can later be catalytically combined into value added chemicals via pathways shown in Fig. 7. We divided the discussion according to the types of halogen source (gaseous halogen, HX, solid metal oxides/oxyhalides and metal halides) while also highlighting a potential of one step halogen/halide facilitated CH_4 activation.

8.2.1. Gaseous halogens for C—H bond activation

Monohalogenmethanes (CH_3Cl or CH_3Br) are analogous to CH_3OH for production of higher hydrocarbons and oxygenates. CH_4 halogenation using gaseous reactants is an example of the oldest electrophilic substitution reaction. Prior to Olah's work on solid superacids, high selectivity to monohalogenated methane, i.e. CH_3X, which is a desired intermediate for further heterogeneous coupling reactions, could only be achieved with CH_4 to halogen

ratio of 10:1 thermally or photochemically [113,114]. Olah used CH_4 and halogen (typically chlorine or bromine) passed through a solid acid catalyst, i.e. $FeO_xC1_y/A1_2O_3$, TaOF,/$A1_2O_3$, $NbOF_3/A1_2O_3$, $ZrOF_2/A1_2O_3$, $SbOF_3/A1_2O_3$, SbF_5/graphite, and Nafion-H/TaF_5) or platinum metal ($Pt/A1_2O_3$ and $Pd/BaSO_4$) at 200–250 °C and atmospheric pressure. These catalysts are highly selective with over 90% selectivity towards monohalogenated methane and conversion of upto 58% [113]. Olah considered the reaction mechanism to consist of the insertion of a surface halogen species or electron-deficient metal site into methane's C—H bond leading to the formation of a five-coordinated carbonium ion followed by bond cleavage to give CH_3X. Some years later, Degirmenci et al., studied homogeneous dibromination of CH_4 [115] and heterogeneous selective CH_4 monobromination over sulfated zirconia catalyst on SBA-15 [116]; the latter is a follow-up study due to the difficulty in converting dibromomethane (CH_2Br_2) into a higher-value product. Their study showed that on 25% sulfated zirconia supported on SBA-15 99% selectivity towards CH_3Br can be achieved with a rather high conversion of ~69%, well above that achieved on Olah's super acid [116]. In general, when dibromomethane (CH_2Br_2) is formed it deposits coke during the following coupling reactions and several attempt were made to address that. First, a small amount of I_2 in the mixture with Br_2 resulted in a very selective monobromination with Br_2 via a secondary (reproportionation) reaction.

$$CH_2Br_2 + CH_4 \rightarrow 2CH_3Br,\ \Delta G_r^\circ(298\,K) = -0.07\,kJ/mol \quad (15)$$

Alternatively, coking problem of dibromomethane (CH_2Br_2) was addressed via Pd_6C/SiO_2 catalyst conversion to higher hydrocarbons and Ru/SiO_2 to convert CH_2Br_2 to CH_3Br [117]. In order to overcome the apparent corrosivity problems of halogen gas reactants as well as the need of halogen regeneration a milder method of CH_4 halogenation was discovered by utilizing oxygen commonly referred to as oxyhalogenation [118–125]. In this method, catalysts can be classified into three groups. Namely, oxides and phosphates [118,120–123], oxyhalides [119,124,125] and metal halide [126–128]. One thing that appears in common with all of these catalysts is that the hydrohalide acid is used to replenish the surface halogen species in accordance with the Mars-van Krevelen mechanism. The reaction involving this mechanism takes place from 200 to 450 °C.

8.2.2. CH_4 oxyhalogenation on metal oxide and phosphate catalysts

Ideally, typical oxyhalogenation yields monohalogenated methane species by the reaction

$$CH_4 + HCl(HBr) + 0.5O_2 \rightarrow CH_3Cl(CH_3Br) + H_2O\ \Delta G_r^\circ(298\,K) = -145.45(-152.59)kJ/mol \quad (16)$$

Various catalysts, mostly rare metal oxides and (oxy)halides, have been shown to perform efficiently including CeO_2 [129] nanoparticles. Metal oxide and phosphate catalyst [118,120–123], as well as Rh/SiO_2 [118] and Ru/SiO_2 [121], are active for the generation of both CO and CH_3Br. These catalysts are designed in a way that both monobromination and partial oxidation of CH_4 take place, yielding CO and CH_3Br, which would be passed on to the next step, to convert them into CH_3COOH. At 560 °C, the Ru/SiO_2 catalyst prepared from $RuCl_3$ attains 30% conversion with ~75% and ~25% selectivity towards CH_3Br and CO, respectively [121]. However, the catalyst is not well-characterized hence it is not clear whether the dopant maintains its chlorinated form or becomes oxide. SiO_2 supported Rh catalyst, on the other hand, can be tuned based on which products are desirable [118]. Calcination of catalyst at higher temperature leads to a lower surface area which heavily favors the formation of CH_3Br, while the opposite is true when a mixture of CO and CH_3Br is desired. *Ex-situ* XPS analysis confirms that the catalyst is in its oxide form even though it was prepared from the chloride precursor and reveals that Rh^{3+} active species is reduced to Rh^0 during the reaction [118]. Metal oxides lacking facile redox ability, such as BaO, can be used to replace the supported Ru and Rh catalyst leading to much more economical catalyst [120]. The catalyst has an improved conversion CH_4 of ~44% with total selectivity toward CH_3OH, CH_3Br, and CO achieving 95% selectivity. The ratio of $CH_3OH + CH_3Br$/CO can be tuned so as to be equal to unite suitably as a feedstock for CH_3COOH production. The problem, however, lies with the deactivation of the catalyst, which originates from aggregation of barium particles, preventing metathesis between BaO and $BaBr_2$ from taking place [120].

Another class of catalyst for oxybromination of CH_4 is based on iron phosphate supported on silica [122,123]. Conversion reached 50% with total selectivity toward CO and CH_3Br of 95%, with the ratio of both main products being equimolar [122]. The reaction mechanism was proposed to follow a redox/free radical mechanism where the phosphate is reduced to Fe^{2+} by HBr, producing $Br^\bullet$ in the process, as confirmed by XRD, XPS and ^{57}Fe Mössbauer spectroscopy. Oxygen plays an important role in reoxidizing the phosphate. The catalyst maintains its activity for about 200 h on-stream time, where catalyst deactivation takes place due to the accumulated CH_2Br_2 that leads to coking [123].

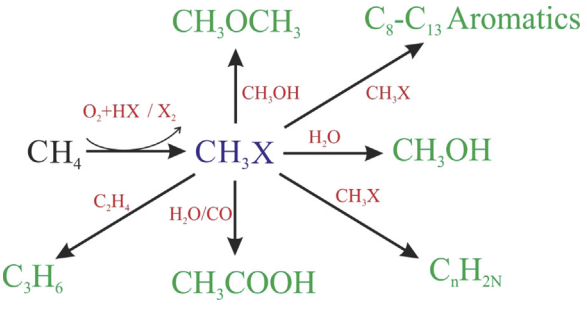

Fig. 7. CH_3X (where X = Cl, Br or I) based routes for CH_4 conversion into value added products.

8.2.3. Oxyhalides for oxychlorination

A special case of oxychlorination catalysts is the oxychloride catalysts, e.g. LaOCl [119,125] and K_4RuOCl_{10}/TiO_2 [124] that are used in a one-pot methyl halide (CH_3X) synthesis from CH_4 with selectivity of »90% and 80%, respectively. Revealed by *in-situ* Raman spectroscopy, $LaCl_3$ in the absence of HCl flow will transform into LaOCl when CH_4 and oxygen are passed through [125]. The catalyst, however, could not maintain its activity dropping to a lower steady-state value. In this case, the reaction was limited by the chlorine atom's bulk diffusion to the surface. The catalyst, similar to metal halides, serves as a halogen source for the oxychlorination of CH_4 with HCl needed subsequently to regenerate the surface [119,125]. In the case of lanthanum oxychloride, the absence of gas-phase oxygen was detrimental to the catalytic activity which implies that oxygen plays a significant role in the reaction. DFT work on the reaction mechanism demonstrated that the oxygen atom dissociates on the surface of $LaCl_3$, thus activating the surface by making an —OCl group that will abstract a proton from CH_4 leaving a hydroxylated, Cl-deficient surface. This surface will be replenished by HCl [125]. Modification of the catalyst with strongly redox active cobalt and cerium chloride leads to a higher concentration of —OCl sites, which leads to the overall higher activity [119]. On the Ru-based catalyst, however, Shalygin et al. reached a different conclusion [124]. Exposure of CH_4 to K_4RuOCl_{10}/TiO_2 at 300 °C demonstrated the formation of $—OCH_3$, carboxylate and carbonyl species, as confirmed by FTIR experiments. The proposed mechanism in this case was different from that of LaOCl catalysts with CH_4 adsorbed on the

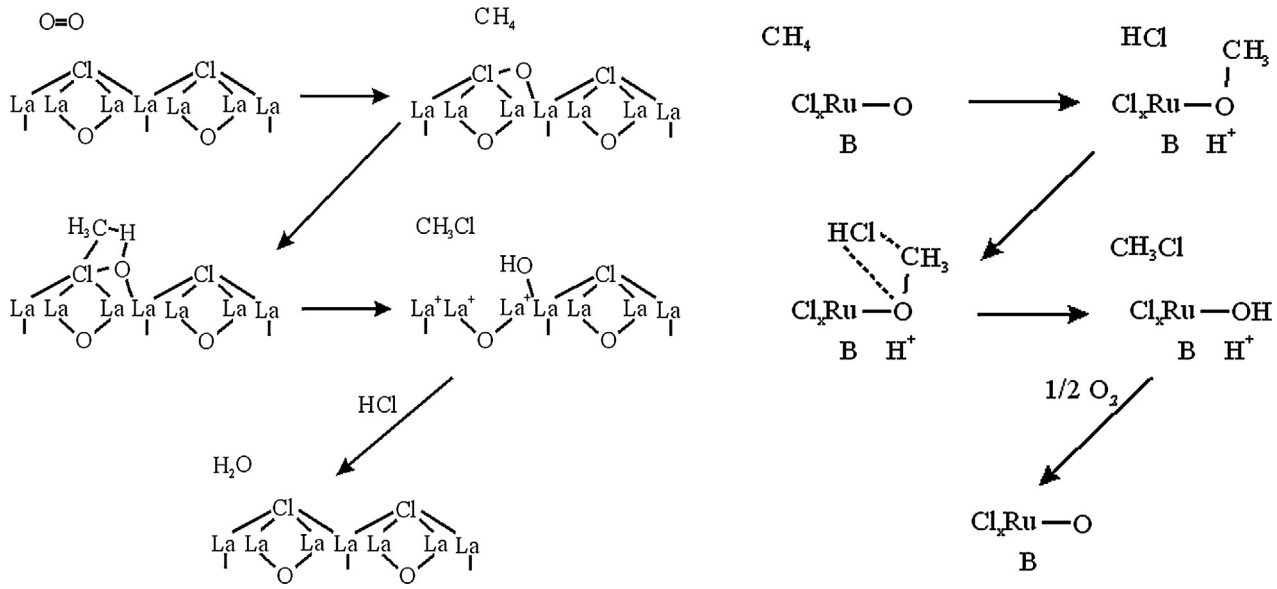

Fig. 8. Two proposed mechanisms for CH_4 oxychlorination on (left) lanthanum oxychloride, involving the formation of —OCl site; (right) on ruthenium-based oxychloride, where CH_4 adsorbs as a surface —OCH_3 species [124,125].

surface as —OCH_3 species, which will be chlorinated by HCl leaving a hydroxylated surface in the process [124]. Fig. 8 contrasts the difference of both mechanisms.

8.2.4. Pure halides for (oxy)chlorination and (oxy)bromination

Lots of complex single step chlorination mechanisms using solid and liquid metal halides have been disclosed for oxychlorination. For example, Taylor and Noceti used $CoCl_2$ catalyst with minor amounts of an alkali metal chloride (KCl) and of a rare earth chloride ($LaCl_3$) achieving 50 and 80% conversion of CH_4 and HCl, respectively [130]. Very similar performance was observed for copper chloride catalyst, which is also active in Deacon chemistry (HCl oxidation to Cl_2). Formic acid was a useful byproduct of partial CH_4 oxidation, too.

A similar concept was applied using metal halides as halogen source and later regenerating it. A very first system was disclosed in US Patent 3,172,915, where $FeCl_3$ was used as a solid catalyst and contacted with CH_4 yielding $FeCl_2$ and CH_3Cl in the process [131]. This first step was then followed by regeneration of $FeCl_3$ and generation of Fe_2O_3 by contacting the reduced metal halide with oxygen/air and HCl.

$$2FeCl3 + CH4 \rightarrow CH3Cl + HCl + 2FeCl2,$$

$$\Delta G_r^{\circ}(298\,K) = 94.72\,kJ/mol, \quad (17)$$

$$FeCl_2 + HCl + 1/4O_2 \rightarrow FeCl_3 + 1/2H_2O, \quad (18)$$

$$FeCl_2 + 1/4O_2 \rightarrow 2/3FeCl_3 + 1/6Fe_2O_3, \quad (19)$$

$$1/6Fe_2O_3 + CH_3Cl + 2(1/2)H_2O \rightarrow CH_3OH + 1/3FeCl_3{\cdot}6H_2O, \quad (20)$$

$$1/3FeCl_3{\cdot}6H_2O \rightarrow 1/3FeCl_3 + 2H_2O \quad (21)$$

It follows that the metal halide catalyst is recycled to the first step, while the oxide is used to further transform the CH_3X into CH_3OH. Another multistep process was also disclosed in US Patent 5,243,098 in a similar manner using $CuCl_2$ and MgO, with the MgO being used to convert the halide into CH_3OH [132].

$$2CuCl_2 + CH_4 \rightarrow CH_3Cl + HCl + 2CuCl, \quad \Delta G_r^{\circ}(298\,K) = -25.88\,kJ/mol, \quad (22)$$

$$H_2O + CH_3Cl + HCl + MgO \rightarrow CH_3OH + MgCl_2{\cdot}H_2O, \quad (23)$$

$$MgCl_2{\cdot}H_2O \rightarrow MgO + 2HCl, \quad (24)$$

$$2CuCl + 2HCl + 1/2O_2 \rightarrow 2CuCl_2 + H_2O, \quad (25)$$

$$MgCl_2 + CuO \rightarrow MgO + CuCl_2, \quad (26)$$

$$CuCl + 1/2Cl_2 \rightarrow CuCl_2. \quad (27)$$

Another similar system, yet not entirely comparable, is the one disclosed in US Patent 5,998,679, where $FeBr_3$ is heated *in-situ* to give off Br_2 gas that would react with CH_4, producing HBr and methyl bromide (CH_3Br) [128]. The HBr is then reacted to $Fe(OH)_3$ to regenerate $FeBr_3$.

$$2FeBr_3 \rightarrow 2FeBr_2 + Br_2 \quad (28)$$

$$CH_4 + Br_2 \rightarrow CH_3Br + HBr, \quad \Delta G_r^{\circ}(298\,K) = -30.94\,kJ/mol \quad (29)$$

$$3CH_3Br + Fe(OH)_3 \rightarrow FeBr_3 + 3CH_3OH \quad (30)$$

$$3HBr + Fe(OH)_3 \rightarrow FeBr_3 + 3H_2O \quad (31)$$

$$12FeBr_2 + 3O_2 + 6H_2O \rightarrow 8FeBr_3 + 4Fe(OH)_3 \quad (32)$$

8.2.5. CH_3X carbonylation to CH_3OH, DME or CH_3COOH

Early utilization of CH_3X was pursued by Olah [133], in which carbonylation was expected to take place over Friedel-Crafts catalysts, such as BF_3, $AlBr_3$, and $AlCl_3$. Carbonylation indeed took place, however, the resulting acetyl halide quickly lost HX, giving off a ketene in the process. The ketene is susceptible to further polymerization, yielding polyketene. The general CH_3X conversion to CH_3COOH would need CO as the co-reactant, which can also be generated *in-situ* along with CH_3X production [118,120–123,134].

For instance, after the generation of CH_3Br and CO over Ru/SiO_2 catalyst the resulting products are reacted with water over $RhCl_3$, a precious metal catalyst, to give 99% CH_3Br conversion and 99% CH_3COOH selectivity [121,134,135]. Addition of potassium iodide (KI) as a co-catalyst would alter the selectivity of the catalyst yielding more dimethyl ether (DME) or CH_3OH. The reaction pathways to CH_3OH, DME and CH_3COOH have been discussed previously, both involving hydrolysis [134,136,137]. On $RhCl_3$ catalyst, *in-situ* FTIR product characterization elucidated the reaction pathway, where a metal site adsorbs two CO molecules before dissociatively adsorbing CH_3X. Rh-CH_3 is subsequently dissociated with one CO molecule abstracting the $-CH_3$ group and yielding acetyl halide, which further desorbs and reacts with water to give CH_3COOH [134]. For CH_3OH synthesis over alumina and zeolites, DFT calculations showed that dissociation of CH_3X by a surface hydroxyl or surface M^+ O^- on an exchanged surface yield a $-OCH_3$ group, which will either react with water to give CH_3OH or with another CH_3OH to couple into DME [136,137]. Metal-doped zeolite catalysts give a rather low conversion, less than 10%, but with >90% selectivity towards CH_3OH [136]. On the other hand, mesoporous alumina gives higher conversion for methanolysis (50%) as opposed to hydrolysis (17%) at 300 °C [137]. Another catalyst used for hydrolysis-methanolysis to DME is $ZnCl_2$ [138]. $ZnCl_2$ supported on silica achieves an initial conversion of about 90% and rapidly loses activity due to Cl^- anion migration to below 50% after just 7 h TOS [138].

8.2.6. CH_3X coupling to higher olefins and aromatics

Apart from conversion to CH_3COOH and CH_3OH, CH_3X has been shown to catalytically couple to give higher hydrocarbons [117,139–151]. Early study by Murray et al., includes the formation of C_2H_4 from CH_3X (I, Cl, Br) over metal-doped zeolites [141,142]. CH_3I, for instance, is coupled to C_2H_4 at 500 K over CsX-zeolite [141]. ^{13}Cs MAS NMR was used to monitor the reaction *in-situ* and revealed $-OCH_3$ and ethoxy simultaneously on CsX zeolite with the ethoxy subsequently desorbing to yield C_2H_4. A mechanism similar to Methanol-to-Olefin (MTO) was proposed where CH_3X dissociated to $-OCH_3$ on the zeolite surface followed by proton transfer, yielding the $-OCH_2$ group. This group is then coupled with a CH_3^+ ion from another CH_3X species before a second proton transfer takes place, releasing C_2H_4 in the process [141]. Different metal dopants provided different selectivities with $Zn^{2+} > Cd^{2+}$ and $Mg^{2+} > Ba^{2+}$, suggesting Lewis acidity plays an important role in the reaction [142]. On Cu-ZSM-5 the reaction exclusively yields C_2H_4 and no other hydrocarbons. Interestingly, the catalysts were not calcined at high temperatures leading to a proposed mechanism, where bases of the metals were present as dopants instead of their oxides [142].

On CaO/ZSM-5 CH_3Br was postulated to react with HBr to yield higher hydrocarbons and water with the oxide is subsequently converted to $CaBr_2$ while still retaining some activity towards CH_3Br [140,152].

$$HBr + CH_3Br + CaO/ZSM\text{-}5 \rightarrow 1/n(C_nH_{2n}) + H_2O + CaBr_2/ZSM\text{-}5 \quad (33)$$

$$CH_3Br \rightarrow HBr + 1/n(C_nH_{2n}) \text{on} \, CaBr_2/ZSM\text{-}5 \quad (34)$$

The resemblance of this reaction to MTO is also confirmed when CH_3Cl and CH_3Br are reacted over H-SAPO34 with a similar product distribution, induction periods and hydrocarbon deposition on the catalyst [153]. The activity of the catalyst reached 60% at 450 °C later decreasing logarithmically reaching only 20% after 8 h time-on-stream (TOS). Both CH_3Cl and CH_3Br exhibited similar activity and selectivity with C_2H_4 and C_3H_6 being the main product at ~50% and ~25% selectivity, respectively [153].

SAPO catalysts were also thoroughly investigated by Su and Liu's groups [144–151]. *In-situ* IR experiments showed alkoxy group as an intermediate, similar to that of MTO, at a reaction temperature of 350 °C [150,151]. Upon adsorbing the CH_3X, Al—O—P bonds break generating large amounts of P—OH groups which are converted back once HCl is desorbed from the surface. At higher CH_3Cl partial pressures conversion increased dramatically suggesting participation of the gas phase in the reaction mechanism [151]. Another mechanistic study using the deuterated molecule, CD_3Cl, and *in-situ* IR resulted in a revised mechanism [146]. Contradicting a previous finding, the deuterated experiment revealed no dissociation of CH_3X during the process, even though there was a weak bonding between the surface hydroxyl group and the halogen group [146]. On SAPO-34 catalysts conversion reached 65% at 500 °C with the total selectivity towards C_2H_4, C_3H_6 and butylene of ~80% [151]. Interestingly, when the reaction temperature increased, lower olefins were more favored as the main products. Incorporation of Mn into the SAPO framework resulted in the formation of an Si island, as confirmed by NMR and FTIR [145]. This catalyst exhibited strong acidity resulting in a higher activity and light olefin selectivity when compared to SAPO-34 catalyst. Mg, Co, and Fe were also studied as potential dopants in the SAPO framework [147,149]. In all these cases activity and selectivity were enhanced with Co favoring C_2H_4 formation with Fe improving both C_2H_4 and C_3H_6 formation [147]. Mg was a slightly different case where incorporation of the alkali earth metal decreased the acidity of the surface and introduced new coordination sites where Al was replaced by Mg in the framework [149]. The addition of Mg results in a milder reaction rate, while also improving catalyst life and selectivity toward C_3H_6 of ~35% with conversion still at ~45% even after 155 h TOS [149]. ZSM-5 had also been investigated as the support for Mg dopant, where the active site was identified to be $MgBr_2$, similar to that reported by Lorkovic et al. [140]. However, this system used both HBr and CH_3Br as reactants with carbon pool as the confirmed mechanism.

Another study aimed at elucidating the reaction mechanism of CH_3X to olefins was also carried out by Olsbye et al. [143]. Just like Su and Liu's groups, the reaction was studied over H-SAPO 34 catalyst and the mechanism was confirmed by an *in-situ* IR and isotopic labeling experiments. The mechanism followed that of MTO, with the main difference being the proton's affinity to the functional group rendering the main obstacle to be thermodynamics, instead of kinetics [143]. Another unusual system studied was co-reaction of CH_3X with olefins such as C_2H_4 to give a methylated olefin, i.e. C_3H_6 [144]. The formation of C_3H_6 was more prominent in the CH_3X—C_2H_4 system in comparison to the C_2H_4—CH_3OH system. Both ZSM-22 and SAPO-34 were active towards this reaction with C_3H_6 selectivity of 60% obtained at lower conversion. In summary, metal dopant effects on the activity/selectivity of CH_3X coupling reactions are of tremendous interest and could benefit from the combined computational/*in situ* studies.

Higher hydrocarbons, e.g. aromatics, are also targeted as a product for methyl halide upgrading. [154,155]. ZSM-5 is particularly active in this reaction, with PbO promoting the activity [155]. The indispensable active sites in this reaction are the zeolite's acid sites, as proven since on catalysts with smaller particle sizes and high numbers of acidic sites, PbO did not exhibit any improved catalytic activity [154]. At 360 °C, the formation of $C_8 - C_{13}$ is prominent in both catalysts, with C_9 being the main product with selectivity of 30–40% at conversion of well above 95% and aromatic selectivity of 30–45%. In agreement with previous findings the reactive mechanism involves hydrocarbo pool, similar to MTO pathway [154,155]. Another unusual system studied was co-reaction of methyl halide

with olefins, such as ethylene, to give a methylated olefin, i.e. propylene [144]. The formation of propylene is more prominent in the CH_3X—C_2H_4 system in comparison with the C_2H_4—CH_3OH system. Both ZSM-22 and SAPO-34 were active for this reaction with propylene selectivity of 60% obtained at lower conversion.

8.2.7. One step oligomerization of CH_4 using solid and liquid metal halides

A two-step halogenation based CH_4 conversion, while almost quantitative, typically suffers from carbon deposition. Usually, carbonaceous deposits are formed when CH_3Br is coupled using metal oxide catalysts via.

$$nCH_3Br \rightarrow C_{n-1}H_{2n} + nHBr + C \quad (35)$$

These carbonaceous deposits need to be reacted back into hydrocarbons via a separate hydrogenation cycle [156] at 533 K and 80 bar. Polyhalogenated products are not converted efficiently, which causes coking and is a drawback for the process. Additionally, a two-step halogenation necessitates two different catalysts, one for intermediate product handling and one for separation. Finally, tremendous amounts of HCl or HBr are generated during the first step of the activation process. One-way CH_4 transformation methods yielding value added products based on halogen activation has thus been explored.

The most notable recent advance is the use of bromide super acids. They were also utilized to oligomerize CH_4 in one step. Vasireddy and coworkers used a gaseous stream of both $AlBr_3$ and HBr to form $H^+AlBr_4^-$ super acid (CH_4:$AlBr_3$:HBr in a molar ratio of 1:0.005:1.32, residence time 60 s, T = 473 to 673 K, P = 1 atm) to achieve nearly 100% CH_4 conversion stable on stream for at least 6 h at 623 K [157]. "Red oil" was observed in the flash drum at the outlet of the reactor due to the mixture of C_6—C_{26} hydrocarbons in $AlBr_3$: HBr presenting catalyst separation and recycling problems. An undeniable advantage of the process is H_2 coproduction.

Hydrocarbon dehydrogenation and coupling reactions using reducible metal halide molten salts were proposed by Shell Oil Co. in the 1960–70 s and present a curious case of an integral CH_4 activation system that has not been widely pursued [158,159]. In particular, iodine/hydrocarbon systems are considered where (1) reaction of oxygen with a metal iodide to give elemental iodine take place followed by (2) reaction of the liberated iodine with the organic reactant (CH_4) to give a dehydrogenated product and HI and (3) reaction of the HI with metal hydroxide to reform metal iodide. Metal oxides that make metal iodide by reaction with iodine species, including but not limited to arsenic, antimony, lead, zinc, cadmium, copper, nickel, cobalt, manganese, calcium, lithium, cerium and rare earth metals have been proposed [158]. CH_4 coupling to produce C_2H_4 and acetylene was used as an example [158], yet most processes seems to target dehydrogenation of higher paraffins, although C—C bond coupling has been demonstrated for higher hydrocarbons [159]. Importantly, this reaction sequence removes equilibrium limitations for the overall process. Recently, this process has been extended to C_2H_6 oxidative dehydrogenation achieving 95% selectivity on molten alkali chloride (LiCl, KCl) supported Dy_2O_3/MgO catalysts [160]. Conventional oxidative coupling of CH_4 using O_2 and N_2O oxidants in molten salts (KCl-$LnCl_3$ and others) has been routinely performed to yield C_2 products where molten salt is needed to stabilize reduced oxygen species, such as peroxides and super oxides at high temperatures (>500 °C) [161]. A reducible metal oxide process operates at lower temperatures (>300 °C) with the potential to avoid a distinct two-step CH_3X based intermediate, but has not yet been fully explored in CH_4 activation/coupling reactions. Finally, if CH_3X route is used for MTO-like process, a large Deacon facility (HCl oxidation to Cl_2) is necessary to cope with the tremendous amounts of hydrogen chloride generated. Emerging ways that address the need for halogen regeneration thus are of utmost importance and should focus on renewable resources (photoelectrochemical HBr splitting to yield H_2 and Br_2, solar light facilitated solid metal halide based catalysis, etc).

9. Catalytic CH_4 aromatization with higher paraffins and olefins

A thermodynamically much more favorable pathway than HDA exists and involves catalytic reaction of CH_4 with higher alkanes and alkenes to yield C_6H_6 and H_2 via [162]

$$2CH_4 + n\text{-}C_4H_{10} \rightarrow C_6H_6 + 6H_2, \ \Delta G^\circ_r(973\,K) = -36.2\,kJ/mol. \quad (36)$$

Here, lower temperatures (823–873 K) are needed to achieve favorable conversion. Use of gallium based catalyst (Ga_2O_3 both supported and unsupported on MFI (ZSM-5)) has been originally attempted with a successful 12–45% conversion of CH_4 in combination with 91–100% conversion of the additives (n-C_4H_8, i-C_4H_8, C_2H_4, C_3H_6, as well as C_3H_8 and n-C_6H_{14}). Selectivity towards coke was reported $\leq$1 wt%, while that towards aromatics was 92 and 94%. Notably, no CH_4 conversion was achieved with the same reaction parameters (H-Ga-Al-MFI catalyst, concentration of CH_4 in feed, 33.3 mol%; space velocity, 6200 $cm^3\,g^{-1}\,h^{-1}$), showing involvement of the higher hydrocarbon reactive intermediates in CH_4 activation. This interesting phenomenon, the catalytic effect of co-fed hydrocarbons on CH_4 conversion, is of specific interest since it can effectively convert CH_4 to aromatic liquids without coking of the catalyst. The reaction mechanism and structure-activity relationships of this novel catalyst system, however, are poorly understood at present and both the thermodynamics and kinetics have been scrutinized extensively, as indicated in the following sections.

9.1. Catalysts used for CH_4 co-reforming with higher hydrocarbons

The highest activity among metal oxides towards C—H (and H—H) bonds splitting results in the presence of supported Cr_2O_3, Ga_2O_3, and ZnO [163]. As such, Ga_2O_3 promoted zeolite materials have been at the forefront of the research due to the aforementioned unprecedented gallium activity towards homolytic C—H bond cleavage, as well as the resulting shape selectivity of the zeolites [164]. Three types of active species have been proposed so far, including charge-compensation of framework aluminum by mononuclear Ga ($[Ga^+]$, $[Ga(=O)^+]$) or di-nuclear species $[Ga_2O_2{}^{2+}]$ [165,166]. Subsequently, the di-nuclear gallium species provide thermodynamically favorable pathways for C—H homolytic splitting and H_2 desorption due to the less basic O sites of $Ga_2O_2{}^{2+}$ [166,167]. Stability of these species in a reducing environment is not known, or at least has not been investigated. The Zn based supported zeolite catalysts exhibit very similar behavior to those of gallium. The consensus appears to be that non-framework incorporated gallium species are necessary to split the C—H bond [168]. Very little to no knowledge about the chemical state of these catalysts exists at the reactive temperatures and pressures, since *in situ* and *operando* spectroscopy measurements at such high reaction temperatures are difficult.

9.2. Mechanisms, kinetics and thermodynamics

Two major types of C—H bond cleavage mechanisms have been proposed: a carbenium route *vs*. homolytic C—H bond cleavage

[162,168–171]. In particular, homolytic C—H bond cleavage via the σ-bond metathesis based transition state is proposed to more likely occur, as opposed to the carbenium mechanism [169]. For example, Al_{III} sites, the most unsaturated and reactive in alumina, result in lower activation barriers (50–80 kJ/mol) towards C—H bond cleavage than those involving carbonium or carbenium ions (typical E_a of 120–150 kJ/mol) [169]. Similarly, several isotope exchange studies (H/D exchange reaction of D_2/alkane mixtures) showed that Zn-BEA displays a much lower activation energy and higher rates of reaction (ca. 2 orders of magnitude) than the corresponding H-zeolite, which clearly shows that the reaction mechanisms are different for the two systems, i.e., carbonium ion for H-BEA *vs.* metal – alkyl intermediates for Zn-BEA [172].

Alkane transformation into lower and higher homologues – alkane metathesis – involves successful cleavage and formation of C—C bonds. The reverse of this process would constitute a situation where CH_4 is reacted with higher hydrocarbons to yield hydrocarbons with successful incorporation of CH_4, e.g. cross metathesis of CH_4 with higher hydrocarbons observed by Choudhary et al. [162] Such a reaction has been attempted using ^{13}C isotope labelling on tantalum hydride supported on silica [173]. In sharp contrast to the homolytic cleavage mechanism discussed previously, the researchers proposed a mechanism based on carbene intermediates and olefin metathesis, which contradicts the earlier reversed from their own earlier proposed mechanism of cleaving the C—C bond system by either σ-bond metathesis or oxidative addition [174]. The presence of the catalyst bi-functionality appears to be a very important requirement when CH_4 is converted in the presence of CH_3OH since both zeolitic Bronsted base and Ga metal acid sites are needed to form penta-coordinated carbocation and/or carbene ions [168].

In contrast to both major mechanisms, other authors proposed the methylation mechanism on Zn/H-BEA using adsorbed $—OCH_3$ species (arising from CH_4) addition to the aromatics formed exclusively from propane prior to the ^{13}C carbon incorporation into the ring structure via scrambling of the carbon atoms in methylbenzenes by way of the ring expansion/contraction mechanism [170,171]. No presence of alkane was necessary for CH_4 activation and no hydride transfer occurred between activated CH_4 and carbenium ions. Only the co-reactions of CH_4 with C_3H_8 were investigated, which is easier to deprotonate and, thus, it is unclear whether the same argument regarding the reaction mechanism stands with C_2H_6. In support, other authors also claim that at temperatures used by Choudhary et al. [162], the CH_4 insertion reaction via hydride transfer is not thermodynamically feasible [175]. For example, opposite results were observed where Naccache et al. reported that H-galloaluminosilicate did not activate CH_4 and that $^{13}CH_4$ could not be inserted into the products such as aromatics in the conversion of C_2H_4/CH_4 or C_3H_6/CH_4 mixtures [175]. Bradford believed that CH_4 conversion was suppressed in the presence of C_2H_6 having a relatively high concentration [176]. Recent thermodynamic modelling showed that in the working temperature region of 673–873 K, net CH_4 production, rather than consumption, is observed due to the cracking of higher hydrocarbons [177]. In conclusion, there is no consensus about the reaction mechanism to date [178].

10. Catalytic methylation with CH_4

Oxidative methylation of non-oxygenated aromatic hydrocarbons with CH_4 in the presence of air at elevated pressure and temperature has been explored since the 1980s. The most commonly used hydrocarbons as co-reactants are toluene (C_7H_8) or benzene (C_6H_6) with acetonitrile receiving less attention [179–190]. In the absence of air (yielding hydrogen instead of water) the reaction becomes highly unfavorable thermodynamically. The extreme reaction conditions, i.e., 700–750 °C and 1–6 atm pressure, suggest that the reaction is a free-radical process with constraints on the overall products' selectivity. As C_6H_6 is carcinogenic, its methylation to yield toluene and higher alkylates, such as mesitylene (1,3,5-trimethylbenzene), as fuel additives, is of interest via

$$CH_4 \xrightarrow{HDA} C_6H_6 \xrightarrow{methylation} toluene, xylene, mesitylene \quad (37)$$

Highly alkylated compound mesitylene is clearly the one that has been under the radar for a while. It has an excellent octane rating and so far has been synthesized via (a) xylene methyl alkylation [191] and (b) acetone (aldol) condensation using aprotic solvents (N-alkyl pyrolidones, dialkyl formamides, and dialkylamides) and strong liquid acids, such as hydrochloric, phosphoric, sulfuric, and acetic [192,193]. Separation issues and the use of rare or liquid components suggest a wide open area for production of mesitylene via heterogeneous catalysis, while use of CH_4 only as feedstock suggests a novel route in clean fuel production.

10.1. Benzene oxidative methylation

Oxidative methylation of benzene using CH_4 and air has been thoroughly investigated by Adebajo's group [194–197]. In their publications, summarized in Adebajo's perspective paper [194], C_6H_6 is shown to be methylated at 400 °C under the presence of CH_4 and air at 6.9 MPa. Tracing experiments were done using GC–MS and $^{13}CH_4$ in a batch reactor with various acidic catalysts, i.e., HZSM-5, CoZSM-5, Cu-beta, and H-beta. Xylenes, ethylbenzene and toluene were produced under this high pressure with selectivities of 15–30%, 10–30%, and 30–50%, respectively [195]. Isotopic experiments confirmed that methyl groups in both xylenes and toluene originated from the labeled CH_4 with the xylenes' and toluene's mass number increasing by two and one CH_4 mass unit, respectively [194]. Furthermore, when the CH_4 and air streams were replaced by nitrogen and hydrogen the conversion dropped from ~10% down to <1% [194]. *Ex-situ* characterization using XRD, FTIR and (MAS) NMR of the catalysts before and after the reaction indicated that the catalysts retained their crystalline structure and that only a small amount of Brønsted acid sites were necessary for the reaction to take place. Furthermore, (MAS) NMR combined with FT-IR spectra showed that all the active catalysts contained additional octahedral framework aluminum in addition to the normal tetrahedral [195].

The presence of transition metal dopants inevitably led to the partial oxidation of CH_4. This can be regarded as the very first step in the postulated reaction mechanism for oxidative methylation of both C_6H_6 and toluene [194]. CH_4 would be converted to CH_3OH and further methylate the aromatic compound to release water as the byproduct. For example, at 400 °C, 6.9 MPa and 4 h reaction time with no removal of residual air, 9.32% conversion of CH_4 was achieved on HZSM-5, decreasing to ~8% when Co, Mn or Cu were incorporated into the catalyst. Additionally, selectivity towards toluene was highest in undoped HZSM-5 with 65.7% and dropped to ~40% when dopants were introduced. However, dopant introduction led to higher selectivities towards ethylbenzene (up to 41% on Mn-ZSM-5 as opposed to 17% on HZSM-5). Selectivity towards xylenes remained very similar on doped and undoped H-ZSM-5 [194]. The conversion of CH_4 and total yields of the methylated products are still relatively low. Elucidation of the active sites via in situ measurements and reaction mechanisms via quantum chemical calculations as these methylation reactions take place are necessary to better understand selectivity governed by specific metal dopants.

10.2. Toluene oxidative methylation

Bi, Mo and Zn along with alkali and alkaline earth metals are known to be the effective catalysts for toluene oxidative methylation. The reaction has been investigated by Ruckenstein's [186,187,189], Kovacheva's [179,180,182–185] and Suzuki [181,198] groups. Watanabe's group was particularly interested in working with 5% NaBr supported on La_2O_3 catalyst with the support synthesized via thermal decomposition of the rare earth metal's oxalate [181,198]. The catalyst operated at 823 K and yielded C_8 molecules, i.e. ethylbenzene and styrene, as well as benzene, stilbene, 1,2-diphenylethane, ethane, and ethylene. The yield of the expected products, ethylbenzene and styrene, reached only 11.6%. The authors also suggested that the reaction pathway involves oxidative cross-coupling between CH_4 and toluene followed by dehydrogenation of ethylbenzene with several side reactions taking place [198].

Ruckenstein's group, on the other hand, explored a much less exotic, super basic catalyst synthesized by promoting an alkali earth metal oxide with a binary alkali metal [186,187,189]. The increased selectivity was attributed to the synergistic increase in surface basicity when two alkali metals were used [187]. Moreover, it was revealed that catalysts that have Rb as a co-dopant did not perform well compared to the other dopant system [186]. A higher C_8 (styrene/ethylbenzene = 1.6) yield of 24.2% was attained with the reaction carried out at 650–850 °C and atmospheric pressure using 5 mol% Na^+ and 5 mol% Cs^+ as the co-dopants [186]. When compared with the series of alkali earth metal oxide supports, Ca and Mg proved to be the best performing catalysts, where CaO support resulted in >40% yield of C_8 products (styrene/ethylbenzene = 2.2) [187]. Ba and Sr oxides did not perform as well due to the stable carbonates that did not decompose at the reaction temperature, which lead to the blockage of the reaction sites. In parallel with the Ruckenstein group's effort, an MgO-based catalyst has been tried with a third metal nitrate being used to further dope the already basic Li/MgO catalyst [190,199,200]. The third metal dopants investigated were Cu, Ce, Pb, Ni, Bi, Tl and Sm. Pb was the most effective metal giving the highest yield of ~20% of C_8 products with Pb/Li/MgO (5:15:80 mol). The catalyst itself is suspected to have a Pb—Li—O non-crystalline material. Unfortunately, the reason why Pb works better than the other third metal dopant was not investigated by this group. When lead phosphate, as opposed to nitrate, was used as a precursor, the previously encountered problem, Pb loss from the sample, was overcome by the stabilizing effect of the phosphate [199].

Kovacheva's group was interested in the use of basic zeolites for oxidative methylation of toluene [179,180,182–185]. Cesium [180,182] and alkali earth metal oxides [179,183,185] were used as zeolite dopants. Cs-promoted NaX was investigated using three methods of doping: impregnation, ion-exchange and solid-phase ion-exchange. The former exhibited the highest yield (16–18%) at 750 °C followed by that obtained on a solid-phase ion-exchange and ion-exchanged NaX, respectively [180]. XRD and IR studies revealed that non-framework species from CsCl is present in the impregnated catalyst, while the ion-exchanged sample exhibited higher CsCl dispersity. The results suggested that the active sites might be associated with the zeolite lattice and the non-framework species, e.g. with CsCl in a crystalline form [180]. The role of the CsCl crystalline phase in the reaction was further highlighted in the case of the $AlPO_4$-5 support, where, compared to ion-exchanged zeolites, the CsCl retained its crystalline structure, as opposed to the finely dispersed Cs surface species in ion-exchanged catalysts [182]. In this comparative study, CO_2 TPD revealed that the basicity of the promoted $AlPO_4$-5 molecular sieve was the weakest in the order CsX > CsY > CsZSM–5 > $CsAlPO_4$-5. The highest performance, ~10%, was also attained for this catalyst with a reaction temperature of 750 °C and air as the O_2 carrier, where the active sites were thought to be the basic sites depending on the Cs location on the catalyst and the Al content as well [182].

Alkali earth metal oxide groups supported on X-zeolites were also proposed as the catalyst with BaO and SrO as the most active dopants [179,183,185]. MgO yielded a well-dispersed Mg species on the surface of the catalyst, which might be the reason why it is less active than the other dopants. BaO and SrO existed in their crystalline phases leading to the suggestion that these phases are indeed the active species [179,185]. The catalytic activity was directly attributed to the overall basicity of the catalyst, also closely related to the dopants' structure on the zeolite surface [183]. Deactivation of these catalysts was attributed to the formation of carbonates on the surface of the catalyst resulting from the reaction of the dopant with CO_2 produced by the side reaction [183]. A maximum yield of 17–19% was attained with Sr and Ba dopants (1.2×10^{-3} mol/g catalyst) with NaX-zeolite (Si/Al = 1.23), when the reaction was carried out at 750 °C [183].

Toluene oxidative methylation carried out over acidic catalysts was also investigated and reviewed by Adebajo [194]. Acidic catalysts, mainly zeolite-based doped with transition metals such as Cu, Co, and Mn, yielded varying product distributions, where benzene and xylenes were the main products for a batch reaction carried out at 400 °C and 6.9 MPa. Typical toluene conversion on the acidic catalysts was around 16–20% with selectivity towards benzene and xylenes varying between 50 and 80% and 20–40%, respectively. On Cu-ZSM-5 catalyst CH_4 conversion was very low at ~8.5%. However, trimethylbenzene, i.e. mesitylene, was detected with a good C_{9+} aromatics selectivity of ~40% showing a viable alternative route to produce mesitylene without acetone condensation. The product distribution suggested an entirely different mechanism taking place in the process with disproportionation and methylation *via* CH_3OH intermediate to be the main mechanisms [194].

Low conversion and yield are still the main problems in both acid- and base-catalyzed oxidative methylation of toluene, e.g., kinetically limited. Basic catalysts tended to yield products of higher value, such as styrene and ethylbenzene, whereas acidic catalysts resulted in alkylation of multiple ring carbons leading to products such as mesitylene. The lack of fundamental molecular level *in-situ* studies in this area opens a possibility for a deeper mechanistic investigation on active sites and reaction pathways for both acid and base-catalyzed oxidative methylation of aromatics using CH_4.

10.3. One pot CH_4 methylation of aromatics derived from alcohols and ethers (CH_3OH, C_2H_5OH, CH_3OCH_3)

In an effort to alleviate the thermodynamic limitation for methane activation, Choudhary et al. reacted CH_3OH and CH_4 simultaneously over metal-doped ZSM-5 zeolites [168,201]. The reaction took place at a temperature <600 °C and yielded ~70% C_{10+} aromatics for Mo-Zn/ZSM-5 in the product stream. C_2H_5OH and DME also afforded appreciable amounts of higher aromatics. Early isotopic labeling experiments revealed that the aromatics contained contributions from both CH_3OH and CH_4, implying that CH_4 acted as an alkylating agent. Zinc proved to be the most important dopant, because its addition dramatically improved the performance of the catalyst with 100% methanol conversion and about 1.19 mol CH_4/mol CH_3OH consumed. Similar work was performed using 2% Ga/5% Mo/ZSM-5 catalyst, but this time with more emphasis on understanding the underlying chemistry [202]. NH_3-TPD and FTIR characterization of the catalysts reveal that the Bronsted acidity of the catalyst was significantly reduced upon doping. This aligned well with the improved selectivity of 88.7% towards aromatics at 15.5% CH_4 conversion with a reaction temperature of 650 °C [202]. In Choudhary's catalyst the addition of Zn might have

decreased the catalyst's acidity even further leading to a highly bifunctional catalyst. Building on Choudary's work, the investigators studied the effect of doping with Zn as well as the kinetic model of the system and suggested 3% Zn-5%Mo to be the optimum dopant composition on ZSM-5 [203]. Optimum methane conversion was achieved at 30.7% with reaction products, mainly ethylene and toluene with a corresponding selectivity of 42% and 25%, respectively. This system remains an interesting research area to pursue due to the relatively small amount of work done and published. One can also see advantages in sustainability of the process as both abundant CH_4 and ethanol derived from biomaterials can be combined, especially in remote agricultural areas where (bio)ethanol monetization is difficult. Reaction mechanisms need to be investigated using *in-situ* experiments and theoretical modelling, which would address the important intermediates and the active sites leading to a rational design of the catalyst. The observations here (CH_4 dissociating at rather high conversion instead of completely reforming alcohols, whose bonds are weaker than that of C—H in CH_4) suggest a completely kinetically controlled process and rely on Zn, Mo and Ga catalytic sites which seem to be very active (and selective) in many CH_4 catalytic conversion mechanisms (HDA, one step acetic acid formation, methyl halide coupling, toluene oxidative methylation and one step CH_4 photochemical reforming with CO_2 (*vide infra*)).

10.4. HCN synthesis from NH_3 and CH_4

Hydrogen Cyanide (HCN) is a very useful reactive intermediate to make adiponitrile (precursor of Nylon 66), methyl methacrylate, cyanuric chloride, sodium cyanide and other chemicals. The synthesis of HCN from ammonia and CH_4 is a well-known process first introduced by Leonid Andrussow at IG Farben, and had been regarded as Andrussow oxidation [204]. CH_4 and ammonia are flown in the presence of O_2 over a platinum catalyst at 1200 °C. The effluent stream contains ~8% of HCN, with water, CO and CO_2 as the most abundant species [204]. Another known process was discovered by Degussa [205]. The reaction is analogous to steam reforming of CH_4, where in this case CH_4 is reacted with ammonia over Pt-based catalyst to give off HCN and H_2 as a valuable by-product. The reactor effluent mixture contains about 20% HCN and ~70% water with the rest being unconverted reactants and to a lesser extent, byproducts from undesired side reactions. This system is more endothermic and hence, is less important industrially, yet it is academically interesting.

The reaction kinetics and mechanisms on Rh and Pt catalysts were comprehensively studied by Hasenberg and Schmidt [206–208]. The absence of oxygen increased the probability of CH_4 reacting with NH_3 increasing its selectivity toward HCN. The kinetics for this reaction are presumed to follow the Langmuir-Hinshelwood mechanism with CH_4 acting as both reactant and catalyst poison [207,208]. This reaction consists of several steps. Namely, decomposition of CH_4 and NH_3 on the catalyst surface and the reaction of the surface carbon with the produced N fragments or radical N, and/or with ammonia itself. UHV surface analysis using Auger electron spectroscopy (AES) also revealed that the active catalyst surface had one monolayer of carbon atoms, which was also responsible for preventing NH_3 full decomposition to N_2 [208]. However, multilayers of carbon hindered the catalyst's activity, as demonstrated when C_2H_4 was introduced instead of CH_4 [207].

When oxygen was introduced into the reactor the HCN yield dropped significantly and NO became the dominant product [206]. NH_3 is oxidized more easily than CH_4, yet, N_2 production did not increase accordingly. The reaction mechanism was altered in the presence of oxygen; the produced NO reacted with CH_4 to give HCN instead of reacting with another molecule of NH_3 to yield water. The Langmuir-Hinshelwood mechanism, however, still prevailed for both reactions, leading to the conclusion that the reaction has two pathways. AES spectroscopy also revealed that when oxygen is added the surface carbon monolayer is reduced significantly [206]. On a separate effort, Suarez and Loffler also concluded that the reaction was dependent on the surface diffusion of CH_4 or surface reaction referring to the Langmuir-Hinshelwood mechanism as well. Interestingly, they also found out that excessive CH_4 introduction resulted in catalyst deactivation, which was basically due to the multilayer carbon coverage on the surface [209]. Interest in the HCN chemistry, the Degussa process in particular, has recently renewed with the focus on deeper understanding of the reaction mechanism [210–212]. An *in-situ* work was conducted using molecular beam mass spectrometry bridging the UHV experiments and the industrial process [210]. In this study, methylamine, CH_3NH_2, and methylenimine, $CH_2 = NH$, were surprisingly detected during the reaction. The experiments failed to capture the existence of free radicals most likely due to their high reactivity. The origin of both CH_xNH_y compounds was proposed to be due to the surface desorption, when the C—N bond is made. At the reaction temperature methylamine easily undergoes pyrolysis to yield methylenimine, which would further dehydrogenate in the gas phase to give HCN and H_2 [210]. Temporal analysis of products (TAP) experiments were conducted when varying the order of the reactant introduction [212]. While HCN was produced rapidly when ammonia was introduced before CH_4, the opposite was true when a CH_4 pulse was introduced before ammonia. The rate determining step, according to these authors, was the decomposition rate of ammonia. Another mechanistic study was conducted theoretically using DFT. The study considered various catalysts, i.e. Ag, Cu, Pt, and Rh, and also the logarithmic turnover frequency (TOF), as well as the coverage effect of both N and C fragments on the catalyst surface [211].

10.5. Other oxidative methylation with CH_4 (acrylonitrile, other oxygenates)

Ruckenstein's group attempted to methylate acetonitrile with their bialkali super basic catalyst [213] to investigate the potential of replacing a conventional C_3H_6 based process with the one that uses widely available CH_4. The catalysts were either CaO or MgO impregnated by either monoalkali or bialkali precursors. Sulfates, hydroxides, chlorides, acetates, carbonates, and nitrates were used as precursors before the catalyst was dried and calcined. The calcination transformed the catalysts into "super basic" oxide catalysts, which, when exposed to CH_4, oxygen and acetonitrile, afforded ~70% selectivity towards acrylonitrile and up to 25% yield at a reaction temperature of 750 °C, 1 atm pressure [213]. CH_4 conversion was a mediocre 12%. The product distribution of the super basic catalyst also included propionitrile, CO and HCN, as well as suggesting at least two reaction pathways taking place in parallel [214]. At this reaction temperature the chain radical mechanism takes place most of the time, deprotonating CH_4 and acetonitrile, which will recombine to give off propionitrile. The resulting C_3 species might further undergo oxidative dehydrogenation and yield acrylonitrile. The presence of HCN, on the other hand, suggests that oxidative disproportionation of acetonitrile could take place [214].

Another group led by Smirniotis took a similar approach on synthesis of this super basic catalyst, employing 15–30% LiO supported on CaO/MgO [215–218]. On the monoalkali-doped surface the secondary reaction, i.e. oxidative disproportionation, did not take place; only the primary reactions took place. Another plausible mechanism was postulated via the Langmuir-Hinshelwood mechanism with the gas-phase oxygen playing an important role in replenishing the lattice oxygen [216]. When the oxygen was used as a limiting reactant, deactivation of the catalyst took place faster and reaction favored the formation of CO and CO_2, since the lattice oxy-

gen was extracted from the surface to help facilitate the complete oxidation [217]. The lack of produced C_2 species in the reactor effluent, normally presumed to originate from two unbounded ($^{\bullet}CH_3$) species, was the basis for the proposed reaction mechanism that entailed two surface species, $-CH_3$ and acetonitrile, reacting to give off the desired product, acrylonitrile.

A second dopant on the catalyst proved to be detrimental to the catalytic performance by increasing its basicity and reducing the activity, ruling out the inclusion of bialkali-doped catalysts as active catalyst [216,218]. On an interesting note the best performing catalyst was synthesized using LiCl [215]. The calcined catalyst possessed both Li^+ and Cl^- ions on the surface maintaining an atomic ratio of 1:1, as confirmed by XPS. The Cl^- ions, however, are the reaction spectators contributing nothing to the reaction itself; it results from the transformation of LiCl into Li^+O^-. Deactivation of the catalyst is a major problem in this case since all active catalysts lost their activity due to the migration of Li^+ out from the catalyst. Interestingly, oxide prepared from lithium nitrate retains its Li^+ content, though not being active for the reaction [215]. Similar to the other cases of oxidative methylation, there is no exact mechanistic study, i.e. *in-situ* work, which supports these authors' claims on reaction mechanisms and active sites. Furthermore, selectivity to acrylonitrile (~30%) is not sufficient, with the formation to CO_2 still being more favorable (~60%) with 50–60% conversion of acetonitrile [215].

Some other oxygenates, such as picolines, acetone and acetophenone, as well as diphenylmethane were also reacted with CH_4 and air over monoalkali/bialkali promoted magnesia catalyst, typical of Ruckenstein's group, yielding their corresponding methylated product [219,220].

11. Light and electron stimulated CH_4 conversion to value products

An extensive review of renewable energy based CH_4 activation is provided elsewhere [19]. Renewable methods based on solar photons or electrons are of big potential in remote areas as they can also address effective transformation and storage of electricity, sometimes generated in excess and difficult to store and distribute otherwise [221]. Similar to the high temperature CH_4 conversion process, however, photoelectrochemical (PEC) processes are chiefly utilizing radical intermediates generated *in situ* and have the corresponding low selectivity of radical initiated and driven reactions.

Analogously, with the conventional CH_4 catalytic conversion, the PEC facilitated processes can be classified as

- the endothermic routes that use photons or electrons to generate radical intermediates from CH_4, solvent (H_2O) and dissolved salts (KCl) to activate C—H bond followed by the recombination of the species.
- the exothermic oxidation route, e.g. using O_2 as the oxidant that liberates the heat of reaction as electrical potential (i.e. fuel cell).

Overall activity of the process typically depends on the semiconducting behavior of the materials and purely photocatalytic processes are generally of very low conversion and activity, whereas direct electrochemical methods inevitably result in the complete oxidation of CH_4. So far these challenges have thwarted any sizeable use of renewable energy for CH_4 conversion and conceptually new routes need to be devised.

11.1. Electrochemical CH_4 activation

Partial electrooxidation of CH_4 was proposed and utilized by Frese, with Au, glassy carbon, Cu and Hg electrodes that were exposed to CH_4 at room temperature [222]. These electrodes perform efficient oxygen reduction to yield various peroxides at low overpotentials (carbon, Hg, and Au) as well as being effective at oxidizing CH_4 via O_2 at the solid/gas interface (Cu). Alkaline conditions were utilized (0.01–2 M KOH, 0.1 M $NaClO_4$ and 2 M NaOH) with electrode potentials ranging from +0.8 to +0.4 V vs. dynamic hydrogen electrode (DHE). Gaseous products measured included CH_2O, CH_3OH, CO and CO_2 with the dominant product being CH_2O. Ogura and Takamagari combined electrochemistry and photochemical oxidation of CH_4 with a 0.6 M KCl solution as an electrolyte to produce CH_3OH, CH_3Cl, and CH_2Cl_2 [223]. Cell potential was varied from 1.1 to 2.0 V at pH 11.0 and a combination of both photochemistry and electrochemistry was used to produce the chlorine molecules, form their radicals and thermally react them to yield chlorinated CH_4 molecules. CH_3Cl appeared to be the dominant product with CH_3OH and dichloromethane (CH_3Cl_2) being the next most common species. These studies were further refined by Ogura et al. [224,225]. They showed that Pt working and counter electrodes at 1.3 V vs. SHE produced CH_3OH, CH_3Cl and CH_2Cl_2 in aqueous electrolyte at pH 11.0 when illuminated for 3 h with a 10 W Hg lamp at 25 °C. The authors proposed that upon the photodissociation of Cl_2 formed electrochemically CH_4 can be converted to CH_3Cl and CH_3OH. The formation of CH_3OH was proposed to be due to the hydrolysis of CH_3Cl. This powerful concept relied on the inherent reactivity of ions in halide aqueous solutions by generating Cl_2 *in situ*, a very interesting although inefficient case of halogen based CH_4 single step activation.

11.2. Photochemical CH_4 activation

CH_4 activation using a combination of deep UV (180–200 nm) provides another way of breaking a very strong C—H bond with or without a surface present [226,227]. C_1 oxygenates were obtained with CH_4 conversion of up to 13% on 1 g of commercial Beta 811 zeolite with formic acid, formaldehyde and CH_3OH in the condensed phase after 1 h irradiation [226]. When O_2 was present as a co-reactant, the oxygenated product selectivity was 95%. The radical based mechanism was confirmed using alternative reactants, such as H_2S. In a theoretical analysis it has been shown to yield reactive HS· and H· radicals in the presence of 200 nm light to reform CH_4 into CH_3SH, an activated CH_4 intermediate [228] that can later be converted in MTO-like process using conventional heterogeneous pathways. However, both types of processes (direct splitting of C—H bonds and external reactant facilitated) are heavily reliant on high energy UV lights and will require large amounts of inexpensive surplus electricity. Ogura et al. examined the photochemical activation of CH_4 in the presence of water, which produced CH_3OH as the dominant product (~70% at 90 °C) followed by formic acid (11%), ethanol (5%), formaldehyde (5%), acetone (4%) and CH_3COOH (3%). This was due to the hydroxyl radical formation from the photolysis of water at temperatures lower than 100 °C [224].

In a halogen inspired (photo)catalytic process, a chlorine radical mediated photocatalytic C—H bond activation on TiO_2/BiOBr photocatalyst has been shown to proceed under visible light ($420 < \lambda < 780$ nm) in the presence of oxygen at room temperature with remarkable selectivities (>85%) towards C(sp^3)-H bond activation [229]. Reaction times, however, were 4–11 h in a batch type reactor using liquid hydrocarbons, and no chlorinated products were detected. This is possibly due to the chlorine radicals formed on a photocatalyst surface acting as a reactive center eventually leading to oxygenated organic compounds. Also, this is different from conventional heterogeneous CH_4 activation using halogens that suffer from poor selectivity.

11.3. Dry (carbon dioxide) photocatalytic reforming of CH_4

Dry photocatalytic reforming of CH_4 proceeds via

$$CH_4 + CO_2 \rightarrow 2CO + 2H_2 (\Delta G(298\,K) = 171\,kJ/mol) \rightarrow \text{hydrocarbons, oxygenates} \quad (38)$$

and typically yields a variety of oxygenated compounds in a single step, different from the conventional dry reforming product of *syngas*. A variety of wide bandgap semiconductors has been used, including β-Ga_2O_3 [230], Cu/CdS-TiO_2/SiO_2 [231], ZrO_2 [232,233], ZnO [234], TiO_2 [235] and copper phthalocyanine modified TiO_2 [236] on stainless steel mesh, as well as on MgO [237]. Low to near ambient temperatures were utilized ranging from 298 to 423 K and conversions up to 33.1% of CH_4 and 27.9% CO_2 were measured after 8 h exposure by Merajin et al. [235] on TiO_2 at 4 atm (45% CO_2:45% CH_4:10% He) using a UV light source of 125 W. A variety of oxygenates and hydrocarbons was reported, including CH_3COOH, C_2H_6, CH_3COCH_3 and CO. However, these experiments are of low practical value since all were done with residence times of hours. In only one case a gas hourly space volume (GHSV) of 200 h^{-1} was reported, whereas other batch experiments were reported to last from 1 to 8 h. A unique catalytic dry photochemical reforming process on non-metal oxides was reported using transition metal chalcogenide photocatalysts [238]. A series of metal sulfides were utilized including RuS_2 in a UV light reactor with a CH_4:CO_2 (50:50%) stream to produce an unspecified mixture of paraffins, olefins and alcohols. However, the overall process efficiency in these PEC based experiments remains an issue. These batch experiments are akin to catalytic oxidative CH_4 coupling, where the GHSVs are an order of magnitude higher (8000–17,000 h^{-1}) [239]. Two intuitive ways that need to be pursued are (a) plasmon resonance enhanced catalysis and (b) metal halide based photocatalytic routes. While the former provides a local temperature increase (heat) due to the resonant oscillation of electrons (which can act to polarize adsorbing molecules and thus affect selectivity), the latter can certainly combine their intrinsic very high quantum yield efficiencies with the inherent halogen reactivity towards CH_4. Attempts can then be made to combine conventional heterogeneous catalysis utilizing catalysts or reactants that also have a strong plasmon or PEC response with light or electron enhanced processes.

12. Conclusions

A range of chemical compounds, both commodity chemicals and fuels, can potentially be synthesized via single step CH_4 catalytic activation, as well as by the extension methods (C_2H_4 oligomerization, CH_4 alkylation of aromatics, etc.). The data summarized here, however, show deep intrinsic fundamental limitations of a single step direct CH_4 conversion to value added products. These include transient thermodynamic limitations due to the CH_4 activation product reactivity as well as the kinetic limitations yielding coke or poor product yields, as in the case of HDA or direct methylation of aromatics with CH_4. Very high temperatures during HDA combined with the need for precise kinetic control to avoid catalyst coking renders it difficult to implement. Direct partial oxidation using oxygen containing oxidizers exhibits the lowest yields of the useful chemicals reported and at this point appear to be important purely from a scientific perspective, while OCM exhibits promise but the understanding of the transformation on most stable catalysts *in situ* is limited. The curious surface facilitated reaction of CH_4 oxidation to CH_3COOH with and without oxidizer molecules present has so far afforded formation rates in the order of μmol g^{-1}cat h^{-1}. Zn, Ga, Mo and Fe appear to be metals that can govern selective transformations of CH_4 as they facilitate C—H bond breaking, especially when combined with the hydride transfer power of ZSM-5 catalyst. Direct (oxidative) methylation catalysts typically do not result in high yields as they are driven mostly by radical processes. A glaring lack of *in situ* work for most of the reactions described can be viewed as inhibiting the fundamental understanding and preventing rational catalyst design. Lower temperature reactions (<500 °C) rely on different fundamental reasons for C—H bond activation and utilize molecules that are less reactive than O_2 and thus more selective, but result in byproducts that need to be regenerated and are typically more corrosive or toxic (Cl_2, HCl, H_2S). Activated CH_4 heterospecies (CH_3X where X = SH, Cl, Br) can undergo a variety of catalytic routes to form many useful chemical products, but the resulting stoichiometric amounts of the related byproducts complicated the overall process. Renewable power driven processes of CH_4 transformation into value products show the same problems as in high temperature radical driven reactions and proceed at very low efficiencies due to the low quantum yields. However, a combination of light enhanced catalytic reactions using conventional catalyst materials based on plasmon resonance or metal halide can provide benefits to the overall process.

Acknowledgments

This manuscript is based on the work presented at AIChE 2015 by the author (Methane to liquids catalysis: in search of a Holy Grail, Frontier Catalysis Research for Methane Conversion to Chemicals II (Invited Talks), AIChE Annual Meeting, November 8–13th, 2015, Salt Lake City, Utah). Program organizers are acknowledged. Partial financial support by Lehigh University is also acknowledged. Mr. Gregory McCarthy is acknowledged for proof reading the manuscript.

References

[1] EIA Annual Energy Outlook 2012,DOE/EIA-0383(2012) (US Energy Information Administration, Washington, DC), 2014.
[2] U.S. Energy Information Administration, Natural gas flared in North Dakota (2010–2016), 2014.
[3] E. McFarland, Unconventional chemistry for unconventional natural gas, Science 338 (2012) 340–342 (80-.).
[4] U.S. Energy Information Administration, Proved Reserves of Natural Gas – International Energy Statistics, (n.d.).
[5] W. Liss, Addressing the challenges along the Shale gas supply chain, Chem. Eng. Prog. 108 (2012) 34.
[6] Y. Chang, X. Liu, P. Christie, Emerging shale gas revolution in China, Environ. Sci. Technol. 46 (2012) 12281–12282.
[7] G.J. Moridis, T.S. Collett, R. Boswell, M. Kurihara, M.T. Reagan, C. Koh, et al., Toward production from gas hydrates: current status, assessment of resources, and simulation-based evaluation of technology and potential, SPE Reserv. Eval. Eng. 12 (2009) 745–771.
[8] D.T. Allen, V.M. Torres, J. Thomas, D.W. Sullivan, M. Harrison, A. Hendler, et al., Measurements of methane emissions at natural gas production sites in the United States, Proc. Natl. Acad. Sci. 110 (2013) 17768–17773.
[9] N. Unger, D.T. Shindell, D.M. Koch, M. Amann, J. Cofala, D.G. Streets, Influences of man-made emissions and climate changes on tropospheric ozone, methane, and sulfate at 2030 from a broad range of possible futures, J. Geophys. Res. Atmos. 111 (2006) 15.
[10] D.T. Shindell, G. Faluvegi, N. Bell, G.A. Schmidt, An emissions-based view of climate forcing by methane and tropospheric ozone, Geophys. Res. Lett. 32 (2005) L04803.
[11] S. Kirschke, P. Bousquet, P. Ciais, M. Saunois, J.G. Canadell, E.J. Dlugokencky, et al., Three decades of global methane sources and sinks, Nat. Geosci. 6 (2013) 813–823.
[12] B.K. Sovacool, Cornucopia or curse? Reviewing the costs and benefits of shale gas hydraulic fracturing (fracking), Renew. Sustain. Energy Rev. 37 (2014) 249–264.
[13] R.A. Field, J. Soltis, S. Murphy, Air quality concerns of unconventional oil and natural gas production, Environ. Sci. Process. Impacts 16 (2014) 954–969.
[14] G. Myhre, D. Shindell, F.-M. Bréon, W. Collins, J. Fuglestvedt, J. Huang, et al., Anthropogenic and natural radiative forcing, in: Climate Change: The Physical Science Basis. Contribution of Working Group I to the Fifth Assessment Report of the Intergovernmental Panel on Climate Change, Cambridge University Press Cambridge, United Kingdom and New York, NY, USA, 2013, pp. 2013.

[15] J.H. Lunsford, The catalytic conversion of methane to higher hydrocarbons, Catal. Today 6 (1990) 235–259.
[16] J.H. Lunsford, Catalytic conversion of methane to more useful chemicals and fuels: a challenge for the 21st century, Catal. Today 63 (2000) 165–174.
[17] R. Horn, R. Schlögl, Methane activation by heterogeneous catalysis, Catal. Lett. 145 (2015) 23–39.
[18] U.S. Energy Information Administration, Few transportation fuels surpass the energy densities of gasoline and diesel, Today in Energy. (n.d.).
[19] J. Baltrusaitis, I. Jansen, J.D. Schuttlefield Christus, Renewable energy based catalytic CH4 conversion to fuels, Catal. Sci. Technol. 4 (2014) 2397–2411.
[20] J.-P. Lange, Economics of Alkane conversion, in: E. Derouane, V. Parmon, F. Lemos, F. Ramôa Ribeiro (Eds.), Sustainable Strategies for the Upgrading of Natural Gas Fundamental Challenges, Oppor. SE – 3, Springer, Netherlands, 2005, pp. 51–83.
[21] J.J. Spivey, G. Hutchings, Catalytic aromatization of methane, Chem. Soc. Rev. 43 (2014) 792–803.
[22] X. Guo, G. Fang, G. Li, H. Ma, H. Fan, L. Yu, et al., Direct, nonoxidative conversion of methane to ethylene, aromatics, and hydrogen, Science 344 (2014) 616–619.
[23] J. Gao, Y. Zheng, J.-M. Jehng, Y. Tang, I.E. Wachs, S.G. Podkolzin, Identification of molybdenum oxide nanostructures on zeolites for natural gas conversion, Science (2015).
[24] B. Christian Enger, R. Lødeng, A. Holmen, A review of catalytic partial oxidation of methane to synthesis gas with emphasis on reaction mechanisms over transition metal catalysts, Appl. Catal. A 346 (2008) 1–27.
[25] Q. Zhu, S.L. Wegener, C. Xie, O. Uche, M. Neurock, T.J. Marks, Sulfur as a selective soft oxidant for catalytic methane conversion probed by experiment and theory, Nat. Chem. 5 (2013) 104–109.
[26] C. Hammond, S. Conrad, I. Hermans, Oxidative methane upgrading, ChemSusChem 5 (2012) 1668–1686.
[27] S. Abelló, D. Montané, Exploring iron-based multifunctional catalysts for Fischer–Tropsch synthesis: a review, ChemSusChem 4 (2011) 1538–1556.
[28] R.A. Periana, D.J. Taube, S. Gamble, H. Taube, T. Satoh, H. Fujii, Platinum catalysts for the high-yield oxidation of methane to a methanol derivative, Science 280 (1998) 560–564 (80-.).
[29] J.P. Lange, K.P. de Jong, J. Ansorge, P.J.A. Tijm, Keys to methane conversion technologies, in: M. dePontes, J.H. Scholtz, M.S. Scurrell (Eds.), Studies in Surface Science and Catalysis, Elsevier, 1997, pp. 81–86.
[30] A. Holmen, Direct conversion of methane to fuels and chemicals, Catal. Today 142 (2009) 2–8.
[31] J. Oró, J. Han, High-temperature synthesis of aromatic hydrocarbons from methane, Science 153 (1966) 1393–1395 (80-.).
[32] F. Solymosi, J. Cserényi, A. Szöke, T. Bánsági, A. Oszkó, Aromatization of methane over supported and unsupported Mo-based catalysts, J. Catal. 165 (1997) 150–161.
[33] R. Ohnishi, Catalytic dehydrocondensation of methane with CO and CO2 toward benzene and naphthalene on mo/HZSM-5 and Fe/Co-Modified Mo/HZSM-5, J. Catal. 182 (1999) 92–103.
[34] J. Gao, Y. Tang, J.M. Jehng, I.E. Wachs, S.G. Podkolzin, Spectroscopic and computational study of supported Cr and Mo oxides on ZSM-5 for methane dehydroaromatization, in: ACS Meeting, San Francisco, CA (August 10–15, 2014), Division of Catalysis Science & Technology (CATL), 2014.
[35] L. Wang, R. Ohnishi, M. Ichikawa, Selective dehydroaromatization of methane toward benzene on Re/HZSM-5 catalysts and effects of CO/CO2 addition, J. Catal. 190 (2000) 276–283.
[36] S.H. Taylor, J.S.J. Hargreaves, G.J. Hutchings, R.W. Joyner, C.W. Lembacher, The partial oxidation of methane to methanol: an approach to catalyst design, Catal. Today 42 (1998) 217–224.
[37] N.R. Hunter, H.D. Gesser, L.A. Morton, P.S. Yarlagadda, D.P.C. Fung, Methanol formation at high pressure by the catalyzed oxidation of natural gas and by the sensitized oxidation of methane, Appl. Catal. 57 (1990) 45–54.
[38] C. Hammond, M.M. Forde, M.H. AbRahim, A. Thetford, Q. He, R.L. Jenkins, et al., Direct catalytic conversion of methane to methanol in an aqueous medium by using copper-promoted Fe-ZSM-5, Angew. Chem. Int. Ed. 51 (2012) 5129–5133.
[39] D. Park, J. Lee, Biological conversion of methane to methanol, Korean J. Chem. Eng. 30 (2013) 977–987.
[40] O. Benlounes, S. Mansouri, C. Rabia, S. Hocine, Direct oxidation of methane to oxygenates over heteropolyanions, J. Nat. Gas Chem. 17 (2008) 309–312.
[41] C. Michel, E.J. Baerends, What singles out the FeO2+ moiety? A density-functional theory study of the methane-to-methanol reaction catalyzed by the first row transition-Metal oxide dications MO(H2O)p2+, M = V-Cu, Inorg. Chem. 48 (2009) 3628–3638.
[42] P.J. Smeets, R.G. Hadt, J.S. Woertink, P. Vanelderen, R.A. Schoonheydt, B.F. Sels, et al., Oxygen precursor to the reactive intermediate in methanol synthesis by Cu-ZSM-5, J. Am. Chem. Soc. 132 (2010) 14736–14738.
[43] A. Zecchina, M. Rivallan, G. Berlier, C. Lamberti, G. Ricchiardi, Structure and nuclearity of active sites in Fe-zeolites: comparison with iron sites in enzymes and homogeneous catalysts, Phys. Chem. Chem. Phys. 9 (2007) 3483–3499.
[44] E.V. Starokon, M.V. Parfenov, L.V. Pirutko, S.I. Abornev, G.I. Panov, Room-temperature oxidation of methane by α-oxygen and extraction of products from the feZSM-5 surface, J. Phys. Chem. C. 115 (2011) 2155–2161.
[45] M. Sun, E. Abou-Hamad, A.J. Rossini, J. Zhang, A. Lesage, H. Zhu, et al., Methane reacts with heteropolyacids chemisorbed on silica to produce acetic acid under soft conditions, J. Am. Chem. Soc. 135 (2013) 804–810.
[46] J.-F. Wu, S.-M. Yu, W.D. Wang, Y.-X. Fan, S. Bai, C.-W. Zhang, et al., Mechanistic insight into the formation of acetic acid from the direct conversion of methane and carbon dioxide on zinc-modified H-ZSM-5 zeolite, J. Am. Chem. Soc. 135 (2013) 13567–13573.
[47] U. Patil, Y. Saih, E. Abou-Hamad, A. Hamieh, J.D.A. Pelletier, J.M. Basset, Low temperature activation of methane over a zinc-exchanged heteropolyacid as an entry to its selective oxidation to methanol and acetic acid, Chem. Commun. 50 (2014) 12348–12351.
[48] A. Oda, H. Torigoe, A. Itadani, T. Ohkubo, T. Yumura, H. Kobayashi, et al., An important factor in CH4 activation by Zn ion in comparison with Mg ion in MFI: the superior electron-accepting nature of Zn2+, J. Phys. Chem. C 118 (2014) 15234–15241.
[49] H.-J. Freund, J. Wambach, O. Seiferth, B. Dillmann, Verfahren zur Herstellung von Essigsäure, DE 4428566C1, 1995.
[50] W. Huang, K.-C. Xie, J.-P. Wang, Z.-H. Gao, L.-H. Yin, Q.-M. Zhu, Possibility of direct conversion of CH4 and CO2 to high-value products, J. Catal. 201 (2001) 100–104.
[51] E.M. Wilcox, G.W. Roberts, J.J. Spivey, Direct catalytic formation of acetic acid from CO2 and methane, Catal. Today 88 (2003) 83–90.
[52] W. Huang, C. Zhang, L. Yin, K. Xie, Direct synthesis of acetic acid from CH4 and CO2 in the presence of O2 over a V2O5-PdCl2/Al2O3 catalyst, J. Nat. Gas Chem. 13 (2004) 113–115.
[53] Y.H. Ding, W. Huang, Y.G. Wang, Direct synthesis of acetic acid from CH4 and CO2 by a step-wise route over Pd/SiO2 and Rh/SiO2 catalysts, Fuel Process. Technol. 88 (2007) 319–324.
[54] J. Wang, C. Liu, Y. Zhang, B. Eliasson, A DFT study of synthesis of acetic acid from methane and carbon dioxide, Chem. Phys. Lett. 368 (2003) 313–318.
[55] A.A. Gabrienko, S.S. Arzumanov, M.V. Luzgin, A.G. Stepanov, V.N. Parmon, Methane activation on Zn 2+ exchanged ZSM-5 zeolites. the effect of molecular oxygen addition, J. Phys. Chem. C (2015) (151013181011002).
[56] K. Narsimhan, V.K. Michaelis, G. Mathies, W.R. Gunther, R.G. Griffin, Y. Román-Leshkov, Methane to acetic acid over Cu-exchanged zeolites: mechanistic insights from a site-specific carbonylation reaction, J. Am. Chem. Soc. 137 (2015) 1825–1832.
[57] F. Cavani, F. Trifirò, Selective oxidation of light alkanes: interaction between the catalyst and the gas phase on different classes of catalytic materials, Catal. Today 51 (1999) 561–580.
[58] S. Arndt, T. Otremba, U. Simon, M. Yildiz, H. Schubert, R. Schomäcker, Mn–Na2WO4/SiO2 as catalyst for the oxidative coupling of methane. What is really known? Appl. Catal. A 425–426 (2012) 53–61.
[59] http://www.siluria.com/, (n.d.).
[60] J. Wu, S. Li, J. Niu, X. Fang, Mechanistic study of oxidative coupling of methane over Mn2O3/Na2WO4/SiO2 catalyst, Appl. Catal. A 124 (1995) 9–18.
[61] S. Li, B.J. Davies, Oxidative coupling of methane over W-Mn/SiO2 catalyst, Chin. J. Chem. 19 (2001) 16–21.
[62] D.J. Wang, M.P. Rosynek, J.H. Lunsford, Oxidative coupling of methane over oxide-supported sodium-manganese catalysts, J. Catal. 155 (1995) 390–402.
[63] A. Malekzadeh, A.K. Dalai, A. Khodadadi, Y. Mortazavi, Structural features of Na2WO4–MOx/SiO2 catalysts in oxidative coupling of methane reaction, Catal. Commun. 9 (2008) 960–965.
[64] J.B. Bates, Raman spectra of α and β cristobalite, J. Chem. Phys. 57 (1972).
[65] A. Palermo, J.P. Holgado Vazquez, A.F. Lee, M.S. Tikhov, R.M. Lambert, Critical influence of the amorphous silica-to-cristobalite phase transition on the performance of Mn/Na2WO4/SiO2 catalysts for the oxidative coupling of methane, J. Catal. 177 (1998) 259–266.
[66] A.G. Dedov, G.D. Nipan, A.S. Loktev, A.A. Tyunyaev, V.A. Ketsko, K.V. Parkhomenko, et al., Oxidative coupling of methane: influence of the phase composition of silica-based catalysts, Appl. Catal. A 406 (2011) 1–12.
[67] Y.T. Chua, A.R. Mohamed, S. Bhatia, Oxidative coupling of methane for the production of ethylene over sodium-tungsten-manganese-supported-silica catalyst (Na-W-Mn/SiO2), Appl. Catal. A 343 (2008) 142–148.
[68] T. Agapie, Selective ethylene oligomerization: recent advances in chromium catalysis and mechanistic investigations, Coord. Chem. Rev. 255 (2011) 861–880.
[69] F. Speiser, P. Braunstein, L. Saussine, Catalytic ethylene dimerization and oligomerization: recent developments with nickel complexes containing P,N-chelating ligands, Acc. Chem. Res. 38 (2005) 784–793.
[70] R. Dorin, M. Ionel, F. Fajula, V. Hulea, Heterogeneous oligomerization of ethylene over highly active and stable Ni-AlSBA-15 mesoporous catalysts, J. Catal. 323 (2015) 76–84.
[71] J. Heveling, C.P. Nicolaides, M.S. Scurrell, Catalysts and conditions for the highly efficient, selective and stable heterogeneous oligomerisation of ethylene, Appl. Catal. A 173 (1998) 1–9.
[72] M.D. Heydenrych, C.P. Nicolaides, M.S. Scurrell, Oligomerization of ethene In a slurry reactor using a nickel (II) – exchanged silica – alumina catalyst, J. Catal. 197 (2001) 49–57.
[73] V. Hulea, F. Fajula, Ni-exchanged AlMCM-41—an efficient bifunctional catalyst for ethylene oligomerization, J. Catal. 225 (2004) 213–222.
[74] M. Lallemand, O.A. Rusu, E. Dumitriu, A. Finiels, F. Fajula, V. Hulea, NiMCM-36 and NiMCM-22 catalysts for the ethylene oligomerization: effect of zeolite texture and nickel cations/acid sites ratio, Appl. Catal. A 338 (2008) 37–43.
[75] M. Lallemand, A. Finiels, F. Fajula, V. Hulea, Catalytic oligomerization of ethylene over Ni-containing dealuminated Y zeolites, Appl. Catal. A 301 (2006) 196–201.

[76] M. Lallemand, A. Finiels, F. Fajula, V. Hulea, Nature of the active sites in ethylene oligomerization catalyzed by Ni-containing molecular sieves: chemical and IR spectral investigation, J. Phys. Chem. C 113 (2009) 20360–20364.
[77] M. Lallemand, A. Finiels, F. Fajula, V. Hulea, Continuous stirred tank reactor for ethylene oligomerization catalyzed by NiMCM-41, Chem. Eng. J. 172 (2011) 1078–1082.
[78] S. Lin, L. Shi, H. Zhang, N. Zhang, X. Yi, A. Zheng, et al., Microporous and Mesoporous Materials Tuning the pore structure of plug-containing Al-SBA-15 by post-treatment and its selectivity for C 16 olefin in ethylene oligomerization, Microporous Mesoporous Mat. 184 (2014) 151–161.
[79] A. Martínez, M.A. Arribas, P. Concepción, S. Moussa, New bifunctional Ni—H-Beta catalysts for the heterogeneous oligomerization of ethylene, Appl. Catal. A 467 (2013) 509–518.
[80] C.P. Nicolaides, M.S. Scurrell, P.M. Semano, Nickel silica-alumina catalysts for ethene oligomerization—control of the selectivity to 1-alkene products, Appl. Catal. A 245 (2003) 43–53.
[81] A. Finiels, F. Fajula, V. Hulea, Nickel-based solid catalysts for ethylene oligomerization – a review, Catal. Sci. Technol. 4 (2014) 2412–2426.
[82] T. Yashima, Y. Ushida, M. Ebisawa, N. Hara, Polymerization of ethylene over transition-metal exchanged Y zeolites, J. Catal. 36 (1975) 320–326.
[83] I.V. Elev, B.N. Shelimov, V.B. Kazansky, The Role of Ni+ Ions in the activity of NiCaY Zeolite catalysts for ethylene dimerization, J. Catal. 89 (1984) 470–477.
[84] L. Bonneviot, D. Olivier, M. Che, Dimerization of olefins with nickel-surface complexes in X-type zeolite or on silica, J. Mol. Catal. 21 (1983) 415–430.
[85] H. Choo, L. Kevan, Catalytic study of ethylene dimerization on Ni(II)-exchanged clinoptilolite, J. Phys. Chem. B 105 (2001) 6353–6360.
[86] A. Penkova, S. Dzwigaj, R. Kefirov, K. Hadjiivanov, M. Che, Effect of the preparation method on the state of nickel ions in BEA zeolites. A study by fourier transform infrared spectroscopy of adsorbed CO and NO temperature-programmed reduction, and X-ray diffraction, J. Phys. Chem. C 111 (2007) 8623–8631.
[87] P.H. Kasai, R.J. Bishop, D. McLeod, Ligand effects on the redox reactions in nickel- and copper-exchanged zeolites, J. Phys. Chem. 82 (1978) 279–285.
[88] M. Kermarec, D. Olivier, M. Richard, M. Che, F. Bozon-Verduraz, Electron paramagnetic resonance and infrared studies of the genesis and reactivity toward carbon monoxide of nickel(1+) ions in a NiCa-X zeolite, J. Phys. Chem. 86 (1982) 2818–2827.
[89] R.Y. Brogaard, U. Olsbye, Ethene oligomerization in Ni-containing zeolites: theoretical discrimination of reaction mechanisms, ACS Catal. (2016) 5b01957 (acscatal.).
[90] M. Golombok, D. Nikolic, Assessing contaminated gas, Hart's E&P Mag. (2008) 73–75.
[91] U.S. Energy Information Administration, United Arab Emirates, International energy data and analysis, accessed May 18, 2015, n.d.
[92] C.M.A.M. Mesters, R.J. Schoonebeek, Process for the manufacture of carbon disulphide and use of a liquid stream comprising carbon disulphide for enhanced oil recovery, CA 2656776C, 2014.
[93] M.A. Araya, S.T. Dubey, Producing oil and/or gas with emulsion comprising miscible solvent, CA 2705199 A1, 2009.
[94] C. Huang, A. T-Raissi, Liquid hydrogen production via hydrogen sulfide methane reformation, J. Power Sources 175 (2008) 464–472.
[95] F. Galindo-Hernández, J.M. Domínguez, B. Portales, Structural and textural properties of Fe2O3/γ-Al2O3 catalysts and their importance in the catalytic reforming of CH4 with H2S for hydrogen production, J. Power Sources 287 (2015) 13–24.
[96] E.J. Miao, Frank Q. Erekson, Method for direct production of carbon disulfide and hydrogen from hydrocarbons and hydrogen sulfide feedstock, US–A9018957, 1998.
[97] D.E. Smith, R.W. Timmerman, Carbon disulfide, in: Kirk-Othmer Encyclopedia of Chemical Technology, John Wiley & Sons, Inc., 2000.
[98] O.Y. Gutiérrez, L. Zhong, Y. Zhu, J.A. Lercher, Synthesis of methanethiol from CS2 on Ni-, Co-, and K-doped MoS2/SiO2 catalysts, ChemCatChem 5 (2013) 3249–3259.
[99] O.Y. Gutiérrez, C. Kaufmann, J.A. Lercher, Synthesis of methanethiol from carbonyl sulfide and carbon disulfide on (Co)K-promoted sulfide Mo/SiO2 catalysts, ACS Catal. 1 (2011) 1595–1603.
[100] C. Chang, A.J. Silvestri, The conversion of methanol and other O-compounds to hydrocarbons over zeolite catalysts, J. Catal. 47 (1977) 249–259.
[101] S.A. Butter, A.T., Jurewicz, W.W. Kaeding, Conversion of alcohols, mercaptans, sulfides, halides and/or amines, (1975).
[102] A.V. Mashkina, V.R. Grunvald, V.I. Nasteka, B.P. Borodin, V.N. Yakovleva, L.N. Khairulina, Decomposition of alkanethiols to dialkyl sulfides and hydrogen sulfide, React. Kinet. Catal. Lett. 41 (1990) 357–362.
[103] I.E. Wachs, Production of formaldehyde from methyl mercaptans, US 5969191A, 1999.
[104] E. Huguet, B. Coq, R. Durand, C. Leroi, R. Cadours, V. Hulea, A highly efficient process for transforming methyl mercaptan into hydrocarbons and H2S on solid acid catalysts, Appl. Catal. B Environ. 134–135 (2013) 344–348.
[105] C. Cammarano, E. Huguet, R. Cadours, C. Leroi, B. Coq, V. Hulea, Selective transformation of methyl and ethyl mercaptans mixture to hydrocarbons and H2S on solid acid catalysts, Appl. Catal. B 156–157 (2014) 128–133.
[106] V. Hulea, E. Huguet, C. Cammarano, A. Lacarriere, R. Durand, C. Leroi, et al., Conversion of methyl mercaptan and methanol to hydrocarbons over solid acid catalysts – a comparative study, Appl. Catal. B 144 (2014) 547–553.
[107] Y. Jin, S. Asaoka, S. Zhang, P. Li, S. Zhao, Reexamination on transition-metal substituted MFI zeolites for catalytic conversion of methanol into light olefins, Fuel Process. Technol. 115 (2013) 34–41.
[108] G.A. Olah, H. Doggweiler, J.D. Felberg, S. Frohlich, M.J. Grdina, R. Karpeles, et al., Onium Ylide chemistry. 1. Bifunctional acid-base-catalyzed conversion of heterosubstituted methanes into ethylene and derived hydrocarbons. The onium ylide mechanism of the C1 to C2 conversion, J. Am. Chem. Soc. 106 (1984) 2143–2149.
[109] J. Baltrusaitis, T. Bučko, W. Michaels, M. Makkee, G. Mul, Catalytic methyl mercaptan coupling to ethylene in chabazite: DFT study of the first CC bond formation, Appl. Catal. B Environ. 187 (2016) 195–203.
[110] J.B. Kimble, J.H. Kolts, Methane conversion, US 4620057A, 1986.
[111] J.R. Anderson, Y.-F. Chang, K.C. Pratt, K. Foger, Reaction of methane and sulfur: oxidative coupling and carbon disulfide formation, React. Kinet. Catal. Lett 49 (2016) 261–269 (n.d.).
[112] L.P. Didenko, V.R. Linde, V.I. Savchenko, Partial catalytic oxidation and condensation of methane by oxygen and sulphur, Catal. Today 42 (1998) 367–370.
[113] G.A. Olah, B. Gupta, J.D. Felberg, W.M. Ip, A. Husain, R. Karpeles, et al., Selective monohalogenation of methane over supported acid or platinum metal catalysts and hydrolysis of methyl halides over y-alumina-supported metal oxide/hydroxide catalysts. A feasible path for the oxidative conversion of methane into methyl alcohol/Di, J. Am. Chem. Soc. 107 (1985) 7097–7105.
[114] G.A. Olah, Electrophilic methane conversion, Acc. Chem. Res. 20 (1987) 422–428.
[115] V. Degirmenci, D. Uner, A. Yilmaz, Methane to higher hydrocarbons via halogenation, Catal. Today 106 (2005) 252–255.
[116] V. Degirmenci, A. Yilmaz, D. Uner, Selective methane bromination over sulfated zirconia in SBA-15 catalysts, Catal. Today 142 (2009) 30–33.
[117] K. Ding, A.R. Derk, A. Zhang, Z. Hu, P. Stoimenov, G.D. Stucky, et al., Hydrodebromination and oligomerization of dibromomethane, ACS Catal. 2 (2012) 479–486.
[118] Z. Liu, W. Li, X. Zhou, Product oriented oxidative bromination of methane over Rh/SiO2 catalysts, J. Nat. Gas Chem. 19 (2010) 522–529.
[119] E. Peringer, M. Salzinger, M. Hutt, A.A. Lemonidou, J.A. Lercher, Modified lanthanum catalysts for oxidative chlorination of methane, Top. Catal. 52 (2009) 1220–1231.
[120] R. Lin, Y. Ding, L. Gong, J. Li, W. Chen, L. Yan, et al., Oxidative bromination of methane on silica-supported non-noble metal oxide catalysts, Appl. Catal. A 353 (2009) 87–92.
[121] K.X. Wang, H.F. Xu, W.S. Li, X.P. Zhou, Acetic acid synthesis from methane by non-synthesis gas process, J. Mol. Catal. A Chem. 225 (2005) 65–69.
[122] R. Lin, Y. Ding, L. Gong, W. Dong, J. Wang, T. Zhang, Efficient and stable silica-supported iron phosphate catalysts for oxidative bromination of methane, J. Catal. 272 (2010) 65–73.
[123] R. Lin, Y. Ding, L. Gong, W. Dong, W. Chen, Y. Lu, Studies on oxy-bromination of methane and coke deposition over FePO 4/SiO2 catalysts, Catal. Today 164 (2011) 34–39.
[124] A. Shalygin, E. Paukshtis, E. Kovalyov, B. Bal'zhinimaev, Light olefins synthesis from C1-C2 paraffins via oxychlorination processes, Front. Chem. Sci. Eng. 7 (2013) 279–288.
[125] S.G. Podkolzin, E.E. Stangland, M.E. Jones, E. Peringer, J.A. Lercher, Methyl chloride production from methane over lanthanum-based catalysts methyl chloride production from methane over, J. Am. Chem. Soc. 129 (2007) 2569–2576.
[126] W.L. Borkowski, J. Paul, E. Oberdorfer, W.H. Seitzer, Preparation of oxygenated methane derivatives, 3172915, 1965.
[127] J.P. Miller, M. Kling, Conversion of methane to methanol, 5243098, 1993.
[128] J. Miller, Methods for converting lower alkanes and alkanes to alcohols and diols, 5998679, 1998.
[129] J. He, T. Xu, Z. Wang, Q. Zhang, W. Deng, Y. Wang, Transformation of methane to propylene: a two-step reaction route catalyzed by modified CeO2 Nanocrystals and zeolites, Angew. Chem. Int. Ed. 51 (2012) 2438–2442.
[130] C.E. Taylor, R.P. Noceti, Oxyhydrochlorination catalyst, (1992).
[131] W.L. Borkowski, J. Paul, E. Oberdorfer, W.H. Seitzer, Preparation of oxygenated methane derivatives, 3172915, 1965.
[132] J.P. Miller, M. Kling, Conversion of methane to methanol, 5243098, 1993.
[133] A. Bagno, J. Bukala, G.A. Olah, Chemistry in superacids. 8. Superacid-catalyzed carbonylation of methane methyl halides, methyl alcohol, and dimethyl ether to methyl acetate and acetic acid, J. Org. Chem. 55 (1990) 4284–4289.
[134] K.X. Wang, H.F. Xu, W.S. Li, C.T. Au, X.P. Zhou, The synthesis of acetic acid from methane via oxidative bromination carbonylation, and hydrolysis, Appl. Catal. A 304 (2006) 168–177.
[135] Y. Fan, D. Ma, X. Bao, Acetic acid from the carbonylation of chloride methane over rhodium based catalysts, Catal. Lett. 130 (2009) 286–290.
[136] D.R. Fernandes, N. Rosenbach, C.J.A. Mota, Catalytic conversion of chloromethane to methanol and dimethyl ether over metal-exchanged zeolite Y, Appl. Catal. A 367 (2009) 108–112.
[137] A. Khaleel, I. Shehadi, A. Al-Marzouqi, Catalytic conversion of chloromethane to methanol and dimethyl ether over mesoporous??-alumina, Fuel Process. Technol. 92 (2011) 1783–1789.
[138] Q. You, Z. Liu, W. Li, X. Zhou, Synthesis of dimethyl ether from methane mediated by HBr, J. Nat. Gas Chem. 18 (2009) 306–311.

[139] Z. Liu, L. Huang, W.S. Li, F. Yang, C.T. Au, X.P. Zhou, Higher hydrocarbons from methane condensation mediated by HBr, J. Mol. Catal. A Chem. 273 (2007) 14–20.
[140] I.M. Lorkovic, M.L. Noy, W.A. Schenck, C. Belon, M. Weiss, S. Sun, et al., Ci oxidative coupling via bromine activation and tandem catalytic condensation and neutralization over CaO/zeolite composites II. Product distribution variation and full bromine confinement, Catal. Today 98 (2004) 589–594.
[141] D.K. Murray, J.W. Chang, J.F. Haw, Conversion of methyl halides to hydrocarbons on basic zeolites: a discovery by in situ NMR, J. Am. Chem. Soc. 115 (1993) 4732–4741.
[142] D.K. Murray, T. Howard, P.W. Goguen, T.R. Krawietz, J.F. Haw, Methyl Halide reactions on multifunctional metal-exchanged zeolite catalysts, J. Am. Chem. Soc. 116 (1994) 6354–6360.
[143] U. Olsbye, O.V. Saure, N.B. Muddada, S. Bordiga, C. Lamberti, M.H. Nilsen, et al., Methane conversion to light olefins—how does the methyl halide route differ from the methanol to olefins (MTO) route? Catal. Today 171 (2011) 211–220.
[144] J. Li, Y. Qi, Z. Liu, G. Liu, D. Zhang, Co-reaction of ethene and methylation agents over SAPO-34 and ZSM-22, Catal. Lett. 121 (2007) 303–310.
[145] Y. Wei, Y. He, D. Zhang, L. Xu, S. Meng, Z. Liu, et al., Study of Mn incorporation into SAPO framework: synthesis, characterization and catalysis in chloromethane conversion to light olefins, Microporous Mesoporous Mat. 90 (2006) 188–197.
[146] Y.X. Wei, D.Z. Zhang, Z.M. Liu, B.-L.L. Su, Mechanistic elucidation of chloromethane transformation over SAPO-34 using deuterated probe molecule: a FTIR study on the surface evolution of catalyst, Chem. Phys. Lett. 444 (2007) 197–201.
[147] Y. Wei, D. Zhang, L. Xu, F. Chang, Y. He, S. Meng, et al., Synthesis, characterization and catalytic performance of metal-incorporated SAPO-34 for chloromethane transformation to light olefins, Catal. Today 131 (2008) 262–269.
[148] Y. Wei, D. Zhang, Z. Liu, B.-L. Su, Methyl halide to olefins and gasoline over zeolites and SAPO catalysts: a new route of MTO and MTG, Chin. J. Catal. 33 (2012) 11–21.
[149] D. Zhang, Y. Wei, L. Xu, F. Chang, Z. Liu, S. Meng, et al., MgAPSO-34 molecular sieves with various Mg stoichiometries: synthesis, characterization and catalytic behavior in the direct transformation of chloromethane into light olefins, Microporous Mesoporous Mat. 116 (2008) 684–692.
[150] Y.X. Wei, D.Z. Zhang, L. Xu, Z.M. Liu, B.L. Su, New route for light olefins production from chloromethane over HSAPO-34 molecular sieve, Catal. Today 106 (2005) 84–89.
[151] Y.X. Wei, D.Z. Zhang, Z.M. Liu, B.L. Su, Highly efficient catalytic conversion of chloromethane to light olefins over HSAPO-34 as studied by catalytic testing and in situ FTIR, J. Catal. 238 (2006) 46–57.
[152] I. Lorkovic, M. Noy, M. Weiss, J. Sherman, E. McFarland, G.D. Stucky, et al., C1 Coupling via bromine activation and tandem catalytic condensation and neutralization over CaO/zeolite composites, Chem. Commun. (2004) 566–567.
[153] S. Svelle, S. Aravinthan, M. Bjorgen, K.P. Lillerud, S. Kolboe, I.M. Dahl, et al., The methyl halide to hydrocarbon reaction over H-SAPO-34, J. Catal. 241 (2006) 243–254.
[154] L. Tao, G.S. Li, S.F. Yin, O.Y. Qiang, S.L. Luo, X.P. Zhou, et al., Synthesis and characterization of H-ZSM-5 zeolites and their catalytic performance in CH3Br conversion to aromatics, React. Kinet. Mech. Catal. 103 (2011) 191–207.
[155] L. Tao, L. Chen, S.F. Yin, S.L. Luo, Y.Q. Ren, W.S. Li, et al., Catalytic conversion of CH3Br to aromatics over PbO-modified HZSM-5, Appl. Catal. A. 367 (2009) 99–107.
[156] N. Osterwalder, W.J. Stark, Direct coupling of bromine-mediated methane activation and carbon-deposit gasification, ChemPhysChem 8 (2007) 297–303.
[157] S. Vasireddy, S. Ganguly, J. Sauer, W. Cook, J.J. Spivey, Direct conversion of methane to higher hydrocarbons using AlBr3-HBr superacid catalyst, Chem. Commun. 47 (2011) 785–787.
[158] N. Maxwell, Dehydrogenation process, (1963).
[159] C.T. Adams, S.G. Brandenberger, J.B. DuBois, G.S. Mill, M. Nager, D.B. Richardson, Dehydrogenation and coupling reactions in the presence of iodine and molten salt hydrogen iodide acceptors, J. Org. Chem. 42 (1977) 1–6.
[160] C.A. Gärtner, A.C. van Veen, J.A. Lercher, Oxidative dehydrogenation of ethane on dynamically rearranging supported chloride catalysts, J. Am. Chem. Soc. 136 (2014) 12691–12701.
[161] J.B. Branco, A.C. Ferreira, A.M.B. do Rego, A.M. Ferraria, G. Lopes, T.A. Gasche, Oxidative coupling of methane over KCl–LnCl3 eutectic molten salt catalysts, J. Mol. Liq. 191 (2014) 100–106.
[162] V.R. Choudhary, A.K. Kinage, T.V. Choudhary, Low-temperature nonoxidative activation of methane over H-galloaluminosilicate (MFI) zeolite, Science 275 (1997) 1286–1288.
[163] J.S.J. Hargreaves, G.J. Hutchings, R.W. Joyner, S.H. Taylor, A study of the methane–deuterium exchange reaction over a range of metal oxides, Appl. Catal. A 227 (2002) 191–200.
[164] Y. Shu, M. Ichikawa, Catalytic dehydrocondensation of methane towards benzene and naphthalene on transition metal supported zeolite catalysts: templating role of zeolite micropores and characterization of active metallic sites, Catal. Today 71 (2001) 55–67.
[165] N. Rane, A. Overweg, V. Kazansky, R. VanSanten, E. Hensen, Characterization and reactivity of Ga+ and GaO+ cations in zeolite ZSM-5, J. Catal. 239 (2006) 478–485.
[166] E.A. Pidko, R.A. van Santen, E.J.M. Hensen, Multinuclear gallium-oxide cations in high-silica zeolites, Phys. Chem. Chem. Phys. 11 (2009) 2893–2902.
[167] E.A. Pidko, R.A. van Santen, Structure-reactivity relationship for catalytic activity of gallium oxide and sulfide clusters in zeolite, J. Phys. Chem. C 113 (2009) 4246–4249.
[168] V.R. Choudhary, K.C. Mondal, S.A.R. Mulla, Simultaneous conversion of methane and methanol into gasoline over bifunctional Ga-, Zn- In-, and/or Mo-modified ZSM-5 zeolites, Angew. Chem. 117 (2005) 4455–4459.
[169] C. Coperet, C—H bond activation and organometallic intermediates on isolated metal centers on oxide surfaces, Chem. Rev. 110 (2009) 656–680.
[170] M.V. Luzgin, V.A. Rogov, S.S. Arzumanov, A.V. Toktarev, A.G. Stepanov, V.N. Parmon, Methane aromatization on Zn-modified zeolite in the presence of a co-reactant higher alkane: how does it occur? Catal. Today 144 (2009) 265–272.
[171] M.V. Luzgin, A.A. Gabrienko, V.A. Rogov, A.V. Toktarev, V.N. Parmon, A.G. Stepanov, The Alkyl and carbenium pathways of methane activation on Ga-modified zeolite BEA: 13C solid-state NMR and GC–MS study of methane aromatization in the presence of higher alkane, J. Phys. Chem. C 114 (2010) 21555–21561.
[172] A. Stepanov, S. Arzumanov, A. Gabrienko, A. Toktarev, V. Parmon, D. Freude, Zn-promoted hydrogen exchange for methane and ethane on Zn/H-BEA zeolite: in situ 1H MAS NMR kinetic study, J. Catal. 253 (2008) 11–21.
[173] D. Soulivong, C. Copéret, J. Thivolle-Cazat, J.-M. Basset, B.M. Maunders, R.B.A. Pardy, et al., Cross-metathesis of propane and methane: a catalytic reaction of C—C bond cleavage of a higher alkane by methane, Angew. Chem. 116 (2004) 5480–5483.
[174] V. Vidal, A. Théolier, J. Thivolle-Cazat, J.-M. Basset, Metathesis of alkanes catalyzed by silica-supported transition metal hydrides, Science 276 (1997) 99–102.
[175] C.M. Naccache, P. Mériaudeau, G. Sapaly, L. Van Tiep, Y. Ben Taârit, Assessment of the low-temperature nonoxidative activation of methane over H-galloaluminosilicate (MFI) Zeolite: a C-13 labelling investigation, J. Catal. 205 (2002) 217–220.
[176] M.C.J. Bradford, M. Te, M. Konduru, D.X. Fuentes, CH4—C2H6—CO2 conversion to aromatics over Mo/SiO2/H-ZSM-5, Appl. Catal. A 266 (2004) 55–66.
[177] P.M. Bijani, M. Sohrabi, S. Sahebdelfar, Nonoxidative aromatization of CH4 Using C3H8 As a coreactant: thermodynamic and experimental analysis, Ind. Eng. Chem. Res. 53 (2013) 572–581.
[178] M. Tian, T.Q. Zhao, P.L. Chin, B.S. Liu, A.S.-C. Cheung, Methane and propane co-conversion study over zinc, molybdenum and gallium modified HZSM-5 catalysts using time-of-flight mass-spectrometry, Chem. Phys. Lett. 592 (2014) 36–40.
[179] P. Kovacheva, K. Arishtirova, S. Vassilev, MgO/NaX zeolite as basic catalyst for oxidative methylation of toluene with methane, Appl. Catal. A 210 (2001) 391–395.
[180] K. Arishtirova, P. Kovacheva, N. Davidova, Effect of preparation of a CsX zeolite catalyst on the oxidative methylation of toluene with methane, Appl. Catal. A 167 (1998) 271–276.
[181] T. Suzuki, K. Wada, Y. Watanabe, Oxidative methylation of toluene with methane over alkali metal bromide loaded rare earth oxides, Appl. Catal. 53 (1989) L19–L21.
[182] P. Kovacheva, K. Arishtirova, N. Davidova, Oxidative methylation of toluene with methane catalyzed by cesium modified molecular sieves, Appl. Catal. A 178 (1999) 111–115.
[183] P. Kovacheva, A. Predoeva, K. Arishtirova, S. Vassilev, Oxidative methylation of toluene with methane using X zeolite catalyst modified with alkali earth oxides, Appl. Catal. A 223 (2002) 121–128.
[184] P. Kovacheva, K. Arishtirova, A. Predoeva, Basic zeolite and zeolite-type catalysts for the oxidative methylation of toluene with methane, React. Kinet. Catal. Lett. 79 (2002) 149–155.
[185] K. Arishtirova, P. Kovacheva, S. Vassilev, BaO/NaX zeolite as a basic catalyst for oxidative methylation of toluene with methane, Appl. Catal. A 213 (2001) 197–202.
[186] A.Z. Khan, E. Ruckenstein, Oxidative methylation of toluene with methane over superbasic catalysts: a selective route to styrene and ethylbenzene through alternative feedstocks, J. Catal. 143 (1993) 1–21.
[187] A. Khan, E. Ruckenstein, A comparative study of oxidative methylation of toluene with methane to styrene and ethylbenzene over bi-alkali-promoted MgO, CaO SrO or BaO, Appl. Catal. A 102 (1993) 233–251.
[188] R. Manivannan, A. Pandurangan, Formation of ethyl benzene and styrene by side chain methylation of toluene over calcined LDHs, Appl. Clay Sci. 44 (2009) 137–143.
[189] E. Ruckenstein, A.Z. Khan, Effects of superbasic catalysts prepared by promoting MgO with Bialkali Metal compounds on the oxidative coupling of methane, J. Catal. 141 (1993) 628–647.
[190] H. Kim, H.M. Suh, H. Paik, Oxidative methylation of toluene with methane over lead-lithium-magnesium oxide catalysts, Appl. Catal. A 87 (1992) 115–127.
[191] K. Griesbaum, A. Behr, D. Biedenkapp, H.-W. Voges, D. Garbe, C. Paetz, et al., Hydrocarbons, in: Ullmann's Encyclopedia of Industrial Chemistry, Wiley-VCH Verlag GmbH & Co. KGaA, 2000, 2016.

[192] J.E. Hurley, Process for the synthesis of mesitylene, US 3413372A, 1968.
[193] J.B. Braunwarth, R.C. Kimble, Preparation of mesitylene by dehydro-condensation of acetone, US 3267165A, 1966.
[194] M.O. Adebajo, Green chemistry perspectives of methane conversion via oxidative methylation of aromatics over zeolite catalysts, Green Chem. 9 (2007) 526–539.
[195] M. Adebajo, Further evidence for the oxidative methylation of benzene with methane over zeolite catalysts, Catal. Commun. 5 (2004) 125–130.
[196] M.O. Adebajo, M.A. Long, R.L. Frost, Spectroscopic and XRD characterisation of zeolite catalysts active for the oxidative methylation of benzene with methane, Spectrochim. Acta. A. Mol. Biomol. Spectrosc. 60 (2004) 791–799.
[197] M.O. Adebajo, R.L. Frost, Oxidative benzene methylation with methane over MCM-41 and zeolite catalysts: effect of framework aluminum, SiO2/Al2O3 ratio, and zeolite pore structure, Energy Fuels 19 (2005) 783–790.
[198] T. Suzuki, K. Wada, Y. Watanabe, Oxidative methylation of toluene with methane over basic oxide catalysts promoted with alkali-metal bromide, Ind. Eng. Chem. Res. 30 (1991) 1719–1725.
[199] H.-M. Suh, H. Kim, H. Paik, Oxidative methylation of toluene with methane over Li/MgO promoted by Pb3(Po4)2, Appl. Catal. A 96 (1993) L7–L11.
[200] H. Kim, Y. Han, H.-M. Suh, H. Paik, Stabilization of Sm2O3 based catalysts in oxidative methylation of toluene, Appl. Catal. A 105 (1993) L135–L139.
[201] V.R. Choudhary, K.C. Mondal, S.A.R. Mulla, Simultaneous conversion of methane and methanol into gasoline over bifunctional Ga-, Zn- In-, and/or Mo-modified ZSM-5 zeolites, Angew. Chem. Int. Ed. 44 (2005) 4381–4385.
[202] S. Majhi, K.K. Pant, Direct conversion of methane with methanol toward higher hydrocarbon over Ga modified Mo/H-ZSM-5 catalyst, J. Ind. Eng. Chem. 20 (2013) 2364–2369.
[203] S. Majhi, P. Mohanty, A.K. Dalai, K.K. Pant, Statistical optimization of process variables for methane conversion over Zn-Mo/H-ZSM-5 catalysts in the presence of methanol, Energy Technol. 1 (2013) 157–165.
[204] L. Andrussow, Über die katalytische oxydation von ammoniak-methan-gemischen zu blausäure, Angew. Chem. 48 (1935) 593–595.
[205] F. Endter, Die technische synthese von cyanwasserstoff aus methan und ammoniak ohne zusatz von sauerst off, Chem. Ing. Tech. 30 (1958) 305–310.
[206] D. Hasenberg, L.D. Schmidt, HCN synthesis from CH4 NH3, and O2 on clean Pt*1, J. Catal. 104 (1987) 441–453.
[207] D. Hasenberg, L.D. Schmidt, HCN synthesis from CH4 and NH3 on platinum*1, J. Catal. 97 (1986) 156–168.
[208] D. Hasenberg, L.D. Schmidt, HCN synthesis from CH4 and NH3 on clean Rh*1, J. Catal. 91 (1985) 116–131.
[209] M.P. Suárez, D.G. Löffler, HCN synthesis from NH3 and CH4 on Pt at atmospheric pressure, J. Catal. 97 (1986) 240–242.
[210] R. Horn, G. Mestl, M. Thiede, F.C. Jentoft, P.M. Schmidt, M. Bewersdorf, et al., Gas phase contributions to the catalytic formation of HCN from CH4 and NH3 over Pt: an in situ study by molecular beam mass spectrometry with threshold ionization, Phys. Chem. Chem. Phys. 6 (2004) 4514–4521.
[211] L.C. Grabow, F. Studt, F. Abild-Pedersen, V. Petzold, J. Kleis, T. Bligaard, et al., Descriptor-based analysis applied to HCN synthesis from NH3 and CH4, Angew. Chem. Int. Ed. 50 (2011) 4601–4605.
[212] S. Delagrange, Y. Schuurman, HCN synthesis from methane and ammonia over platinum, Catal. Today 121 (2007) 204–209.
[213] E. Ruckenstein, A.Z. Khan, Selective formation of acrylonitrile via oxidative methylation of acetonitrile with methane over superbasic catalysts, J. Chem. Soc. Chem. Commun. (1993) 1290–1292.
[214] E. Ruckenstein, Synergistic effects of superbasic catalysts on the selective formation of acrylonitrile via oxidative methylation of acetonitrile with methane, J. Catal. 145 (1994) 390–401.
[215] C.L. Bothe-Almquist, R.P. Ettireddy, A. Bobst, P.G. Smirniotis, An XRD, XPS, and EPR study of Li/MgO catalysts: case of the oxidative methylation of acetonitrile to acrylonitrile with CH4, J. Catal. 192 (2000) 174–184.
[216] P.G. Smirniotis, W. Zhang, Study of the oxidative methylation of acetonitrile to acrylonitrile with CH4 over Li/MgO catalysts, Appl. Catal. A 176 (1999) 63–73.
[217] W. Zhang, P.G. Smirniotis, Study of oxide-based catalysts for the oxidative transformation of acetonitrile to acrylonitrile with CH4, J. Catal. 182 (1999) 70–81.
[218] W. Zhang, P.G. Smirniotis, Natural gas conversion V, in: Proceedings of the 5th International Natural Gas Conversion Symposium, Elsevier, 1998.
[219] B.M. Reddy, E. Ruckenstein, Oxidative methylation of organic compounds with methane over alkali promoted MgO catalysts, Appl. Catal. A 121 (1995) 159–167.
[220] E. Ruckenstein, B.M. Reddy, Oxidative methylation of α-, β- and γ-picolines with methane vinylpyridines and ethylpyridines over mono- and bialkali promoted magnesia catalysts, Catal. Lett. 29 (1994) 217–224.
[221] Q. Schiermeier, Renewable power: Germany's energy gamble, Nat. (London, U.K.) 496 (2013) 156–158.
[222] K.W. Frese, Partial electrochemical oxidation of methane under mild conditions, Langmuir 7 (1991) 13–15.
[223] K. Ogura, K. Takamagari, Direct conversion of methane to methanol, chloromethane and dichloromethane at room temperature, Nature 319 (1986) 308.
[224] K. Ogura, M. Kataoka, Photochemical conversion of methane, J. Mol. Catal. 43 (1988) 371–379.
[225] K. Ogura, C.T. Migita, Y. Ito, Combined photochemical and electrochemical oxidation of methane, J. Electrochem. Soc. 137 (1990) 500–503.
[226] F. Sastre, V. Fornés, A. Corma, H. García, Selective, room-temperature transformation of methane to C1 oxygenates by deep UV photolysis over Zeolites, J. Am. Chem. Soc. 133 (2011) 17257–17261.
[227] F. Sastre, V. Fornés, A. Corma, H. García, Conversion of methane into C1 oxygenates by deep-UV photolysis on solid surfaces: influence of the nature of the solid and optimization of photolysis conditions, Chem. A Eur. J. 18 (2012) 1820–1825.
[228] J. Baltrusaitis, C. de Graaf, R. Broer, E.V. Patterson, H2S-Mediated thermal and photochemical methane activation, ChemPhysChem 14 (2013) 3960–3970.
[229] R. Yuan, S. Fan, H. Zhou, Z. Ding, S. Lin, Z. Li, et al., Chlorine-radical-mediated photocatalytic activation of C—H bonds with visible light, Angew. Chem. Int. Ed. 52 (2013) 1035–1039.
[230] L. Yuliati, H. Itoh, H. Yoshida, Photocatalytic conversion of methane and carbon dioxide over gallium oxide, Chem. Phys. Lett. 452 (2008) 178–182.
[231] D. Shi, Y. Feng, S. Zhong, Photocatalytic conversion of CH4 and CO2 to oxygenated compounds over Cu/CdS–TiO2/SiO2 catalyst, Catal. Today 98 (2004) 505–509.
[232] Y. Kohno, T. Tanaka, T. Funabiki, S. Yoshida, Reaction mechanism in the photoreduction of CO2 with CH4 over ZrO2, Phys. Chem. Chem. Phys. 2 (2000) 5302–5307.
[233] T. Tanaka, Y. Kohno, S. Yoshida, Photoreduction of carbon dioxide by hydrogen and methane, Res. Chem. Intermed. 26 (2000) 93–101.
[234] G. Mahmodi, S. Sharifnia, F. Rahimpour, S.N. Hosseini, Photocatalytic conversion of CO2 and CH4 using ZnO coated mesh: effect of operational parameters and optimization, Sol. Energy Mater. Sol. Cells 111 (2013) 31–40.
[235] M.T. Merajin, S. Sharifnia, S.N. Hosseini, N. Yazdanpour, Photocatalytic conversion of greenhouse gases (CO2 and CH4) to high value products using TiO2 nanoparticles supported on stainless steel webnet, J. Taiwan Inst. Chem. Eng. 44 (2013) 239–246.
[236] N. Yazdanpour, S. Sharifnia, Photocatalytic conversion of greenhouse gases (CO2 and CH4) using copper phthalocyanine modified TiO2, Sol. Energy Mater. Sol. Cells 118 (2013) 1–8.
[237] K. Teramura, T. Tanaka, H. Ishikawa, Y. Kohno, T. Funabiki, Photocatalytic reduction of CO2 to CO in the presence of H2 or CH4 as a reductant over MgO, J. Phys. Chem. B 108 (2003) 346–354.
[238] R.R. Chianelli, B. Torres, Photochemical processes and compositions for methane reforming using transition metal chalcogenide photocatalysts, US20130239469 A1, 2013.
[239] N. Yaghobi, The role of gas hourly space velocity and feed composition for catalytic oxidative coupling of methane: experimental study, J. King Saud Univ. Eng. Sci. 25 (2013) 1–10.